Educational model of cardiovascular system

A.A. de Goede and A. Schaafsma

Introduction

Investigation and modelling of the cardiovascular system has been a subject of scientific research since ancient times. Whereas physicians were mainly looking for causes and treatments of cardiovascular diseases (CVDs), many physicists, engineers and mathematicians were intrigued by the functioning of the system.[1] Nowadays, modelling of blood flow through the human circulatory system is still an important area of research.[1–3] Relevance of these cardiovascular models is emphasised by the prevalence of CVDs, like atherosclerosis and heart failure. CVD's are the number one cause of death in the developed countries[2–6] and the incidence is predicted to further increase by the ageing population.[5,6] Since most CVDs are associated with altered blood flow patterns, knowledge of the blood flow distribution in arterial blood vessels under normal and pathological conditions is indispensable for diagnostics and treatment.[1–3] In addition, cardiovascular models are often used for the development and evaluation of medical devices, planning of vascular surgeries, outcome prediction of interventions and educational or training systems.[3,7,8]

Many years of research have resulted in a large amount of different cardiovascular models, varying in complexity from zero-dimensional (0D) lumped models, to higher order (up to three-dimensional (3D)) distributed models.[1,9] Model choice and dimensionality selection depends on the aim and required accuracy or degree of detail of the application.[1,10,11]

Figure 1 shows how, for example, the blood flow *(Q)* in a blood vessel is modelled in each dimension. 0D lumped models assume a uniform distribution of blood flow over the entire blood vessel at any moment in time, while higher dimensional distributed models enable variation of blood flow in space.[1,10] For one-dimensional (1D) models this means that in addition to time *(t)*, blood flow can vary over another dimension; for example it may vary over the length *(x)* of the blood vessel. At the same moment in time, blood flow can be high at the proximal end of the blood vessel and low at the distal end. For two-dimensional (2D) models, blood flow can vary over two other dimensions; for example it may vary in addition to length *(x)* also over the height *(y)* of the blood vessel. This makes it possible to model laminar flow (parabola); blood flow is low at the top and bottom of the blood vessel and high in the middle.[12] For 3D models, blood flow can vary over all the three dimensions of the blood vessel: length *(x)*, height *(y)* and width *(z)*. This makes it possible to model laminar flow (cone); blood flow is low near the vessel wall and high at the vessel centre.[1,10,12]

Depending on the research objective, combinations of models can be made.[1] In these so called multiscale models, 0D, 1D, 2D and/or 3D models are coupled to create a complete representation of the cardiovascular system. The different scales of models are represented by their own mathematical characteristics.[10] Our cardiovascular model is an example of such a multiscale model, as the heart compartment is modelled by a 0D lumped model and the vascular tree of blood vessels by a 1D distributed model.
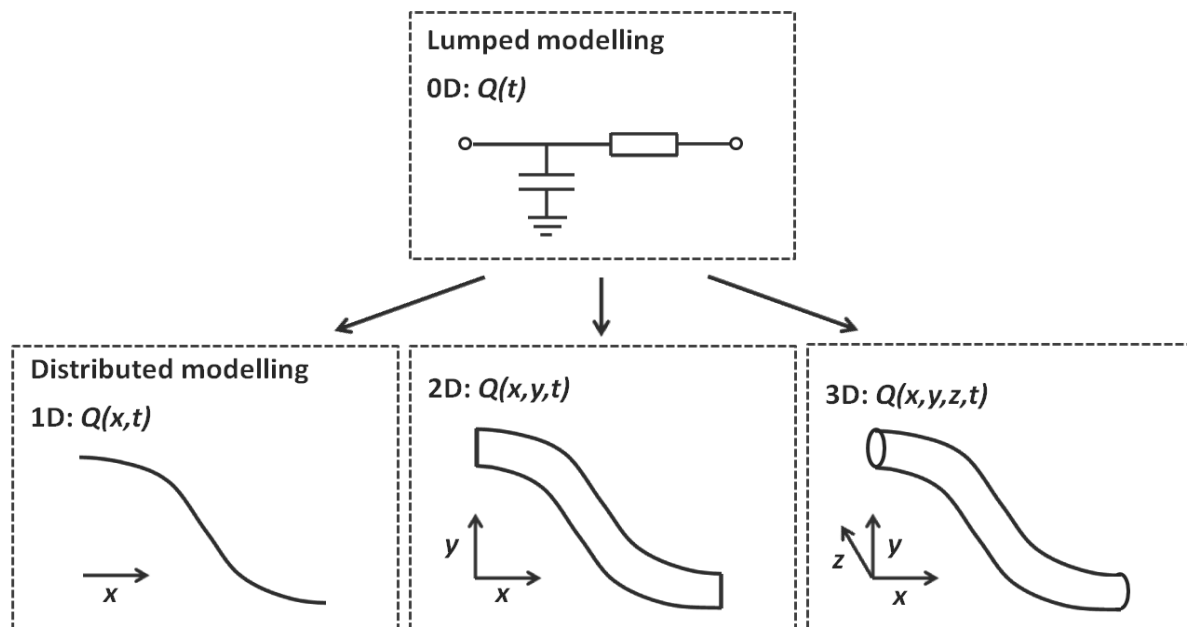
Figure 1. Modelling of blood flow (Q) in different dimensions (0D: lumped modelling; 1D, 2D and 3D: distributed modelling).

0D lumped models describe global hemodynamics of the entire arterial system. As these 0D models assume a uniform distribution of pressure, flow and volume within each compartment (heart, heart valves and arterial blood vessel tree) at any instance in time,[10] they cannot be used to investigate phenomena that occur inside the arterial tree, like wave propagation and reflections.[1,9] A well-known lumped model is the Windkessel model, which considers the entire arterial tree as a parallel combination of total arterial capacitance and total peripheral resistance analogous to electrical circuits.[1,2] The advantage of lumped models is that only a few parameters are needed to describe the main properties of the cardiovascular system.[1] Therefore they are often used to provide boundary conditions for more complex models.[10]

1D distributed models describe local flow and pressure distribution, and their pulse wave propagation through the cardiovascular system.[1,2,13] They are often used to investigate flow and pressure changes along the full length of arterial blood vessels, especially the aorta and larger systemic arteries.[10,14] Dividing the arterial tree into smaller segments of which the mechanical properties and geometry are known makes it possible to describe the pulse wave propagation characteristics of each segment.[1] 1D models owe their value to their low computational complexity combined with their accurate description of flow and pressure distribution.[1,13]

2D and 3D distributed models are used to obtain a detailed description of the local flow or pressure field in a specific part of the cardiovascular system with complex fluid dynamics, like in the heart ventricles, around heart valves, a stenosis or a stent, near bifurcations, or within an aneurysm.[1,10,15] Whereas 2D models are still applicable for axisymmetric structures, most of the time 3D models are required.[14] The computational complexity of 2D and 3D dimensional models limits the extent of the investigation area; it is still only possible to investigate local phenomena and not pulse wave propagation through the entire arterial vessel tree.[1,10,13–15]

THE CARDIOVASCULAR SYSTEM

The main function of the cardiovascular system is the distribution and transportation of blood through the entire circulatory system. Blood circulation is essential to convey nutrients to, and remove waste products from, all the different organs and tissues.[1,2,10,12] Secondary functions include: 1) fast chemical signalling to cells via circulating neurotransmitters and hormones, 2) dissipation of heat from the body core to the surface, and 3) mediation of inflammatory and host defence responses against invading microorganisms.[12]

The cardiovascular system consists of three major components, namely a pump (the heart) that circulates a liquid (the blood) through a system of branching tubes (the vascular tree of blood vessels).[1,2,10,12] Blood is pumped by the heart into the aorta and pulmonary artery, to return via the vena cava and pulmonary vein. In

between blood is distributed over a branching tree-like structure of arteries, arterioles and capillaries, followed by a merging inverse tree-like structure of venules and veins, see figure 2 right bottom.[12] The first part of the vascular blood vessel tree (arterial system) consists of arteries and arterioles and can be regarded as the distribution system, because it provides transportation of blood to organs and tissues. The middle part (microcirculation) of capillaries can be regarded as the diffusion and filtration system, because this is where uptake of nutrients and release of waste products by organs and tissues takes place. While the final part (venous system) of venules and veins can be regarded as the collection system, because it stores blood and returns it to the heart.[1,10,12] The cardiovascular system of humans is divided into two separated circulatory systems; the pulmonary or small circulation and the systemic or large circulation. The former pumps deoxygenated blood to the lungs to deposit carbon dioxide (CO_2) and take up oxygen (O_2), returning oxygenated blood to the heart.[3,12] While the systemic circulation pumps oxygenated blood to the organs and tissues, returning deoxygenated blood to the heart.
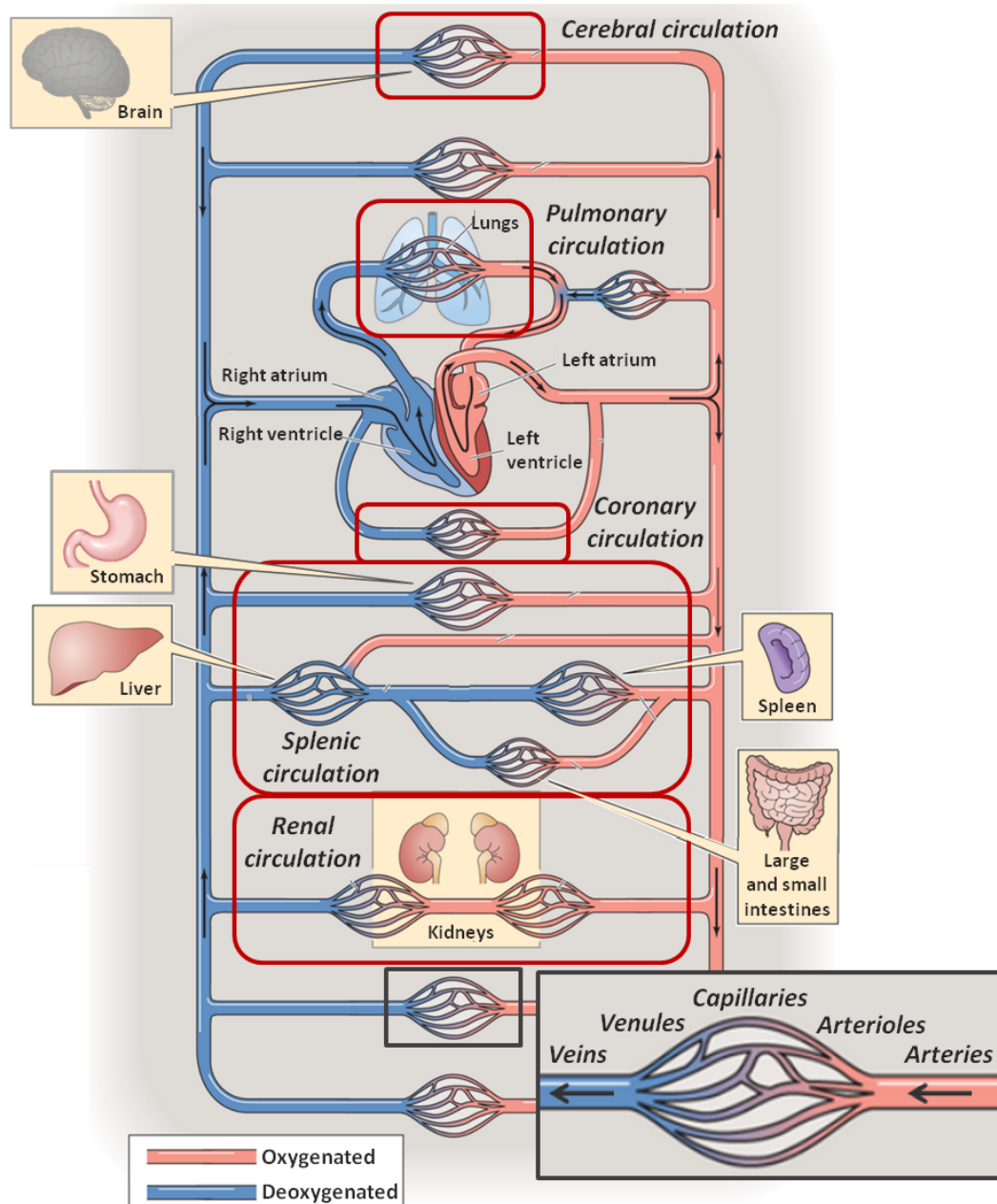

Figure 2. Representation of the different circulatory systems. Right bottom: detailed representation of branching vessel tree-like and merging tree-like structures. Adapted from Medical Physiology (Boron and Boulpaep).[12]

The systemic circulation contains many parallel circulatory systems, like the coronary (heart), cerebral (brain), splenic (stomach, intestines, pancreas, spleen and liver) and renal (kidneys) circulation, see figure 2.[12]

The human circulatory system does not only include a cardiovascular system circulating blood through the body, but also a lymphatic system circulating lymph. Uptake of nutrients and release of waste products by organs and tissues requires exchange of these constituents between blood and tissue cells. This exchange proceeds via interstitial fluid surrounding tissue cells. Interstitial fluid forms in the microcirculation at the arteriolar end of the capillaries and is almost completely (90%) reabsorbed at the venular end of the capillaries. To prevent a build up of interstitial fluid surrounding the tissue cells, the lymphatic circulation removes the remaining 10% of interstitial fluid. In contrast to the cardiovascular system, the lymphatic system contains no pump and is an open system. Lymph is formed in the tissue spaces where lymph capillaries collect the interstitial fluid excess. Via the lymphatic system, lymph finally returns to the venous blood system replacing the volume lost during interstitial fluid formation.[12,16]

IMPLEMENTATION OF THE CARDIOVASCULAR SYSTEM INTO THE MODEL

In agreement with the foregoing, the main components of our cardiovascular model are 1) a heart compartment that pumps 2) blood into 3) a vascular tree of blood vessels. As this cardiovascular model intends to provide insight into systemic and intracranial hemodynamics, the pulmonary circulation is not taken into account. Additionally, as blood flow velocity is measured in the major intracranial arteries during a transcranial Doppler (TCD) measurement, the focus is on the arterial system. Thus the microcirculation and venous system are taken together and represented by a lumped compartment rather than by an inverse branching tree-like structure. Furthermore, the distributed arterial tree is divided into an intracranial (cerebral circulation) part and an extracranial (remaining systemic circulation) part. This makes our cardiovascular model a concatenation of different compartments representing the heart, a branching tree-like structure representing the intracranial circulation parallel to a branching tree-like structure representing the extracranial circulation, and the microcirculation & venous system, see figure 3. As we intend to model blood flow through the cardiovascular system, the lymphatic system is disregarded. It is assumed that the formed interstitial fluid is reabsorbed for 100% in the microcirculation and no lymph is formed in tissue spaces.
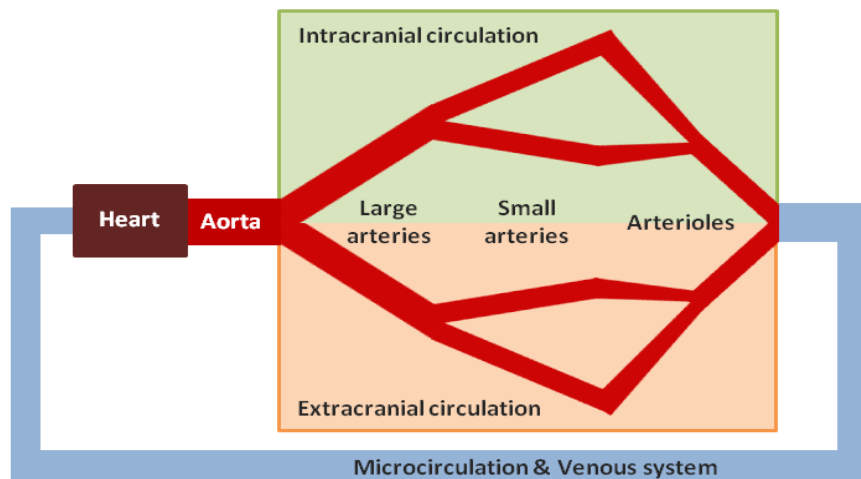

Figure 3. Representation of the cardiovascular system implemented into the model. The vascular blood vessel tree is simplified as a concatenation of straight hollow tubes, with varying diameters.

THE HEART COMPARTMENT

The heart is essential for blood circulation as it delivers the energy needed to distribute and transport blood through the entire circulatory system.[1,12] The heart should be considered as a pulsatile energy generator with an intrinsically regulated frequency; the heart rate (HR). In contrast to other rhythmical behaviours, such as respiration and temperature, which are regulated in the brain, the pacemaker cells of the heart mainly initiate

cardiac contraction itself.[12] The reciprocal of HR is cardiac cycle duration, or heart period,[12,17] which can be divided into two phases: the systole or ejection phase and the diastole or filling phase.[2,3,6,12] During systole the heart pumps a certain amount of blood, the stroke volume (SV), into both the systemic and pulmonary circulation, while during diastole the heart relaxes allowing it to fill again with blood.[12] This means that heart volume is maximal at the end of the diastolic phase and minimal at the end of the systolic phase.

The heart consists of four chambers; a right and left atrium and ventricle. The left ventricle pumps oxygenated blood via the aorta into the systemic circulation, while the right ventricle pumps deoxygenated blood via the pulmonary artery into the pulmonary circulation, see figure 2.[3,6,12] Each ventricle has an inlet or atrioventricular (AV) valve and an outlet or semilunar valve, maintaining the direction of blood flow.[10,12] These cardiac valves open passively when upstream pressure exceeds downstream pressure, and close passively when downstream pressure exceeds upstream pressure.[12] At systolic onset, both the AV and semilunar valves are closed. Due to ventricular contraction, upstream ventricular pressure exceeds downstream aortic and pulmonary pressure, and both AV valves open. Now blood is pumped out of both ventricles. In the beginning, ventricular pressure continues to rise, followed by a rapid elevation of downstream pressures. These rising pressures are accompanied by a precipitous reduction of volume and a fast increase in ventricular outflow. After the first rapid ventricular ejection, both upstream and downstream pressures decrease. As a result, ventricular outflow diminishes and the decline in volume attenuates during the decreased ventricular ejection phase. Eventually ventricular outflow reaches zero, as the closed semilunar valves prevent filling of the heart during systole. At the moment downstream pressure exceeds upstream pressure, both AV valves close, indicating the transition to diastole. Due to the inertia of the blood minimal backflow is seen during closing of the AV valves, resulting in the dicrotic notch or incisura.[12] During diastole ventricles are filled again with blood. Due to the closed semilunar valves no blood is ejected during diastole.[2,3,6,12] Timing of valve opening and closing is not exactly equal for both ventricles, as pulmonary artery pressure (~15 mmHg) is much lower compared to aortic pressure (~95 mmHg). As a result, pulmonary valve opens slightly earlier than aortic valve, while it closes slightly later, making ejection from the right ventricle last a bit longer than that from the left.[12]

Whereas both ventricles operate as mechanical pumps, the atria operate more as passive reservoirs receiving blood from the vena cava (right atrium) and pulmonary vein (left atrium).[12]

IMPLEMENTATION OF THE HEART COMPARTMENT INTO THE MODEL

Since our cardiovascular model does not intend to study interactions between heart mechanics and systemic hemodynamics, no complex heart model is chosen. Based on our choice to focus on the systemic circulation, and thus to leave the pulmonary circulation out of consideration, the heart is modelled by just the left ventricle, the mitral (inlet) valve and the aortic (outlet) valve.

The left ventricle, which should be considered as a volume pump, is modelled by a 0D lumped model that pumps blood into the aorta by a prescribed ventricular outflow curve.[1] During systolic phase mitral valve is closed and aortic valve open, while during diastole mitral valve is open and aortic valve closed, preventing outflow and allowing inflow of blood.[2,3,6,12] Figure 4, shows a standard left ventricular outflow curve (red curve), obtained from measurements in humans. At systolic onset, left ventricular outflow is equal to diastolic outflow; 0 mL/s. After a fast increase towards approximately 500 mL/s, left ventricular outflow gradually declines beginning at around one-third to one-sixth of the systole, to become briefly negative at the transition between systole and diastole.[1,12,18] After some small fluctuations at the transition, left ventricular outflow remains 0 mL/s during the rest of diastole.[12] Different functions are proposed to approximate the left ventricular outflow curve. For example, trapezoidal or rectangular functions are used for the systolic part of the outflow curve when only a rough estimation of systolic outflow is needed.[19,20] However, for a more detailed description either a sinusoidal[14,18–21] or triangular function[17,22,23] is commonly used. An advantage of the triangular curve is that the moment of maximum flow can be easily selected and adjusted,[22] while the abrupt transitions are a disadvantage. The opposite is true for the sinusoidal function; although the moment of peak flow is fixed halfway systole, flow changes gradually along the curve.
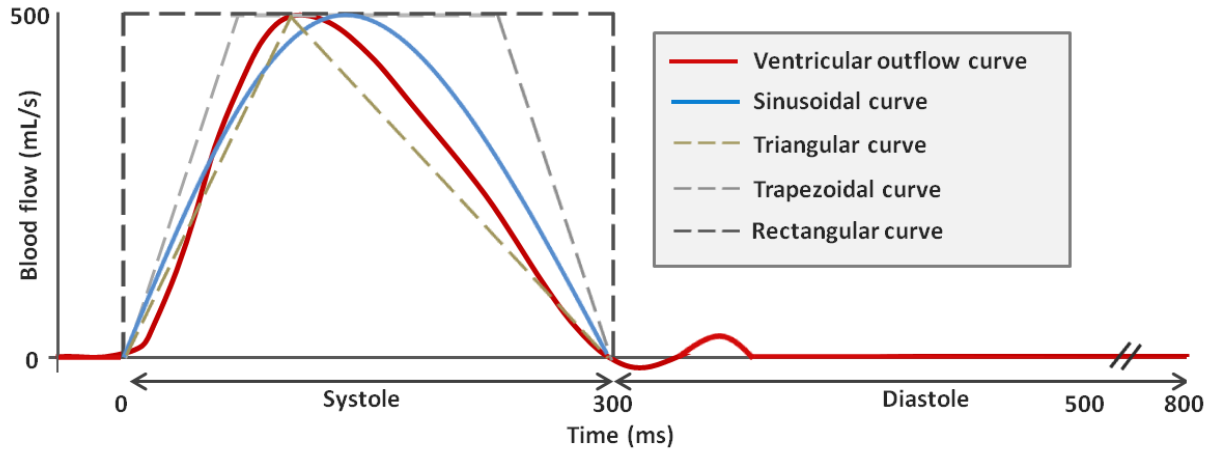
Figure 4. Standard left ventricular outflow curve given in red.[48] Estimated curves for systolic part: sinusoidal curve in blue, triangular curve in brown (dashed), trapezoidal curve in light grey (dashed) and rectangular curve in dark grey (dashed).

In this model we have chosen to model the systolic part of the left ventricular outflow (Q_{out}) curve by a sinusoidal function and the diastolic part by a constant function of 0 mL/s (Equation 1). No retrograde flow or fluctuations at the transition between systole and diastole are modelled, due to the limited added value of these phenomena and to maintain the simplicity.

$$Q_{out} = \sin x \cdot \frac{1}{2} SV \cdot \frac{\pi}{T} \qquad during\ systole \qquad with\ x = \left(\frac{t}{T}\right) \cdot \pi$$
$$Q_{out} = 0 \qquad during\ diastole \tag{1}$$

$t = time$
$T = duration\ of\ systole$
$SV = stroke\ volume$

From this left ventricular outflow function automatically follows the function describing the decline in heart volume, as the amount of volume (V) pumped by the heart into the systemic circulation, during each cardiac cycle, corresponds to the area under the ventricular outflow curve (Equation 2).[12]

$$Q = \lim_{\Delta t \to 0} \frac{\Delta V}{\Delta t} = \frac{dV}{dt} \tag{2}$$

According to equation 2, the function of the volume pumped out of the heart (V_{out}) each cardiac cycle can be obtained by integrating flow over time (Equation 3).

$$V_{out} = -\cos x \cdot \frac{1}{2} SV \qquad during\ systole \qquad with\ x = \left(\frac{t}{T}\right) \cdot \pi$$
$$V_{out} = 0 \qquad during\ diastole \tag{3}$$

$t = time$
$T = duration\ of\ systole$
$SV = stroke\ volume$

For the left ventricular inflow (Q_{in}), our model assumes that the amount of volume flowing out of the microcirculation & venous system flows immediately into the left ventricle, taking into account that this is only possible during diastole (Equation 4). In fact, this is a simplification of reality, as blood from the venous system flows not directly into the left ventricle, but reaches first the left atrium. However, atrial contraction has no significant role in ventricular filling or ejection, and is thus disregarded.[12]

$$Q_{in} = 0 \qquad during\ systole$$
$$Q_{in} = Q_{venous} \qquad during\ diastole \tag{4}$$

According to equation 2, the function of the volume flowing into the heart (V_{in}) each cardiac cycle can be obtained by integrating flow over time (Equation 5).

6

$$V_{in} = 0 \qquad\qquad during\ systole$$
$$V_{in} = V_{venous} \qquad\quad during\ diastole \tag{5}$$

The amount of volume flowing into the heart during diastole becomes the left ventricular SV. This volume is pumped out of the heart during the consecutive systole.[7]

PARAMETER CHOICE - HEART COMPARTMENT

The initial parameter conditions chosen in this cardiovascular model are all based on an adult male person, with a weight of 75 kg. A normal resting HR for this fictitious person is 75 beats per minute (bpm), corresponding to a heart period of 0.8 s or 800 ms.[4,12] Systole and diastole are not equally distributed over the heart period; the duration of systole is about 300 ms, while diastole takes approximately 500 ms.[4,12,14,23] However, percentage duration of systole with respect to total duration of heart period *(systolic fraction(%))* is not fixed and depends on the HR (in bpm); diastole shortens relatively more in comparison to systole with an increasing HR[12,24] (Equation 6).[24]

$$Systolic\ fraction(\%) = 0.01e^{\left(4.14 - \frac{40.76}{HR}\right)} \tag{6}$$

In accordance with total heart volume, left ventricular volume is maximal at the end of diastole and minimal at the end of systole. This makes left ventricular stroke volume (SV_{LV}) the difference between left ventricular end-diastolic volume (EDV_{LV}) and left ventricular end-systolic volume (ESV_{LV}) (Equation 7).[12,25]

$$SV_{LV} = EDV_{LV} - ESV_{LV} \tag{7}$$

It is difficult to find normal values for EDV_{LV} and ESV_{LV}, as both volumes vary with age and gender. Higher values are found in males compared to females and in adults compared to elderly.[25,26] However, EDV_{LV} is on average approximately 120 mL and ESV_{LV} 50 mL, resulting in a SV_{LV} of 70 mL.[4,12] This SV of 70 mL combined with a HR of 75 bpm leads to a cardiac output (CO) of 5.25 L/min or 87.5 mL/s (Equation 8).[7,12]

$$CO = HR \cdot SV \tag{8}$$

In our model the minimal amount of left ventricular volume (ESV_{LV}) is fixed on 50 mL, while EDV_{LV} can vary as it depends on left ventricular inflow. However, EDV_{LV} cannot exceed 190 mL, corresponding to a SV_{LV} of twice the initial condition.

Table 1. Initial parameter conditions - heart compartment.

Parameter	Initial condition	Remarks
Heart rate (HR)	75 bpm	
Heart period	800 ms	
Duration systole	291.8 ms	~300 ms
Duration diastole	508.2 ms	~500 ms
Left ventricular stroke volume (SV_{LV})	70 mL	Maximum limited to 140 mL
Left ventricular end-diastolic volume (EDV_{LV})	50 mL	Fixed
Left ventricular end-systolic volume (ESV_{LV})	120 mL	Maximum limited to 190 mL
Cardiac output (CO)	5.25 L/min or 87.5 mL/s	

THE BLOOD COMPARTMENT

In the cardiovascular system, blood functions as the carrier fluid conveying nutrients to and removing waste products from all the different organs and tissues.[2,12] Blood is a complex mixture composed of formed elements or blood cells (~45%) and blood plasma (~55%).[2,3,12] Blood contains three types of formed elements, namely 1) red blood cells (erythrocytes), important for the transportation of O_2 and CO_2, 2) white blood cells

(leukocytes), important for the human immune response, and 3) blood platelets, important for blood coagulation.[3,12] Blood plasma is an aqueous solution (92% water) containing plasma proteins, carbohydrates, lipids and ions.[2,12] Strictly speaking blood is not a fluid, but a suspension of particles in a fluid called blood plasma.[3] Blood is approximately three times more viscous than water, due to the presence of blood cells increasing blood viscosity and affecting fluid behaviour.[2] Whereas blood plasma is still very nearly Newtonian,[12] whole blood is non-Newtonian.[1,12,15] A fluid has a constant viscosity and is thus homogenous or Newtonian, if the relationship between shear stress and shear rate is linear and goes through the origin.[12] The fact that blood is non-Newtonian means that some threshold force should be applied before blood will move, making it immobile at low forces (for example in the microcirculation).[12] However, at higher forces, which are normally seen in the arterial system, blood acts like a Newtonian fluid.[2,12,15]

Humans have a total blood volume of approximately 5000 mL,[12] which is not equally distributed over the cardiovascular system. Approximately 250 mL (5%) is located in the heart, approximately 500 mL (10%) in the pulmonary circulation and the remaining 4250 mL (85%) in the systemic circulation. This latter 4250 mL of blood that resides in the systemic circulation can be further subdivided into approximately 3250 mL (75%) - or ~65% of total blood volume - located in the venous system. Approximately 250 mL (6.25%) - or ~5% of total blood volume - in the microcirculation, and the remaining 750 mL (18.75%) - or ~15% of total blood volume - in the arterial system,[12] see figure 5a. Another way to subdivide the total volume of 5000 mL over the cardiovascular system is by making a distinction between the heart containing approximately 250 mL (5%), the high-pressure system containing approximately 750 mL (15%) and the low-pressure system containing 4000 mL (80%), see figure 5b. Here the high-pressure system includes the arterial system of systemic circulation, and the low-pressure system the microcirculation and venous system of systemic circulation along with the entire pulmonary circulation.[12] Both of the volume distributions show clearly the effect of the distributing properties of the arterial system (small volume) and the collecting properties of the venous system (large volume).
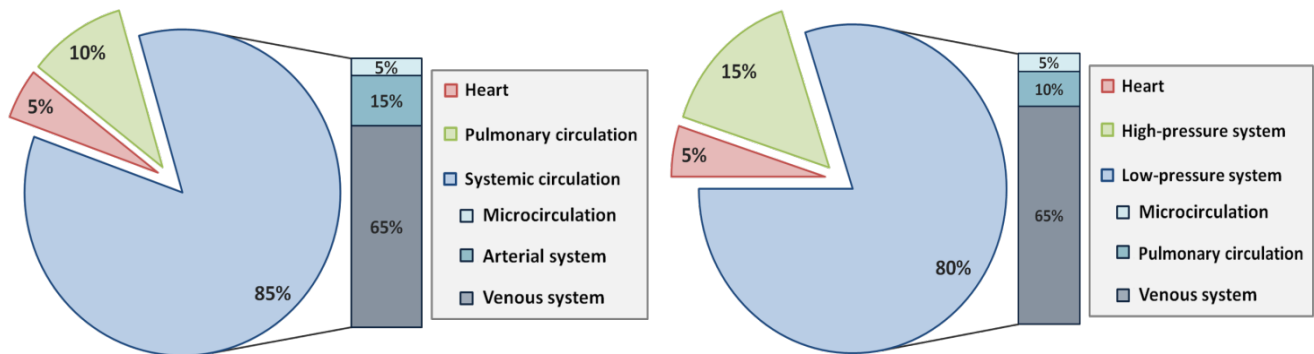

Figure 5a. Volume distribution option 1: heart (red), pulmonary circulation (green) and systemic circulation (blue).

Figure 5b. Volume distribution option 2: heart (red), high-pressure system (green) and low-pressure system (blue).

IMPLEMENTATION OF THE BLOOD COMPARTMENT INTO THE MODEL AND PARAMETER CHOICE

Due to our focus on the high pressure arterial system, we consider blood as a Newtonian fluid with a constant viscosity of 0.0032 Pa·s (0.0032 (kg/m·s)).[12,15,18] The total blood volume of 5000 mL is distributed over the different compartments as follows: 250 mL (5%) in the heart compartment, 500 mL (10%) in the pulmonary circulation, 750 mL (15%) in the arterial system of systemic circulation (high-pressure system) and 3500 mL (70%) in the microcirculation & venous system of systemic circulation.[12]

Normally, the heart volume of 250 mL is distributed over the four heart chambers. As our heart compartment is modelled by only a left ventricle containing 120 mL at systolic onset, an isolated volume container of 130 mL is implemented representing the remaining heart volume. In addition, another isolated volume container of 500 mL is implemented representing the pulmonary circulation, as this part of the cardiovascular system is also not taken into account. Both of these volume containers are not interacting with the cardiovascular model. They

are only adjusted in case of blood loss or blood excess. By making use of these isolated volume containers the initial total blood volume is 5000 mL, just as in normal human beings.

The arterial system, our area of interest, can be further subdivided into arteries containing 600 mL (80%) of blood and arterioles containing 150 mL (20%).[12] Furthermore, the arterial system of this model consists of a part representing the intracranial (cerebral) circulation parallel to a part representing the extracranial circulation. It is well known that although the brain only weighs 2% of the total body weight, it receives 15% of the CO and it accounts for 20% of the glucose consumption. Thus, the brain is well vascularised, in order to meet the relatively large need of blood supply.[12,27] For our fictitious person of 75 kg, it means that his brain weights 1.5 kg (normal range 1 - 1.5 kg).[12] In addition to white and grey matter, the brain contains approximately 150 mL of cerebrospinal fluid and 150 mL of blood. Around 30 mL (20%) of the 150 mL blood is located in the arterial system, while the microcirculation & venous system contain the remaining amount of volume (120 mL).[28,29] This knowledge allows us to deduce that of the total amount of 750 mL present in the arterial system, up to 30 mL (4%) is located inside the brain and thus in the intracranial circulation.

Table 2. Initial parameter conditions - blood compartment.

Parameter	Initial condition	Remarks
Viscosity *(η)*	0.0032 Pa·s or 0.0032 kg/m·s	Newtonian fluid
Total blood volume	5000 mL	
• Heart	250 mL	5% of total blood volume
• Pulmonary circulation	500 mL	10% of total blood volume
• Systemic circulation	4250 mL	85% of total blood volume
o Arterial system	750 mL	18.75% or 15% of total blood volume
• Arteries	600 mL	80% of arterial blood volume
• Arterioles	150 mL	20% of arterial blood volume
o Microcirculation	250 mL	6.25% or 5% of total blood volume
o Venous system	3500 mL	75% or 65% of total blood volume
Percentage intracranial	4%	
Percentage extracranial	96%	

THE VASCULAR TREE OF BLOOD VESSELS

A complex tree-like structure, such as the vascular tree of blood vessels, is essential for transportation of blood to and from all the different organs and tissues, even the most remote ones. The vascular tree consists of a tree-like branching structure of aorta, arteries, arterioles and capillaries, followed by an inverse tree-like structure of venules, veins and vena cava, see figure 2 right bottom. In this complex vascular tree each particular level of arborisation has its unique characteristics and physical properties. The amount of parallel vessels of each successive level in the tree-like structure increases tremendously from a single aorta into billions of capillaries, accompanied by a decline in individual vessel radius and cross-sectional area.[10,12] However, a fundamental law of vessel branching states that the aggregated cross-sectional area of all parallel child vessels should always exceed the cross-sectional area of the parent vessels.[10,12,15] For the inverse tree-like structure the opposite is true; the amount of parallel vessels of each successive level decreases, accompanied by an increase in individual vessel radius and cross-sectional area. See table 3.

Table 3. Characteristics of vascular tree of blood vessels.

Arborisation level	Number of units (N)	Internal vessel radius (r)	Cross-sectional area $(A = \pi \cdot r^2)$	Aggregate cross-sectional area $(A_{total} = N \cdot \pi \cdot r^2)$
Aorta	1	11.3 mm	4 cm^2	4 cm^2
Arteries	8000	0.5 mm	$7.9 \cdot 10^{-3}$ cm^2	63 cm^2
Arterioles	$2 \cdot 10^7$	0.015 mm	$7.1 \cdot 10^{-6}$ cm^2	141 cm^2
Capillaries	$1 \cdot 10^{10}$	0.003 mm	$2.8 \cdot 10^{-7}$ cm^2	2827 cm^2
Venules	$2 \cdot 10^7$	0.01 mm	$3.1 \cdot 10^{-6}$ cm^2	63 cm^2
Veins	8000	0.4 mm	$5.0 \cdot 10^{-3}$ cm^2	40 cm^2
Vena cava	1	13.8 mm	6 cm^2	6 cm^2

The wall of all blood vessels consists of three layers: 1) the tunica intima or inner layer of endothelial cells facing the blood, 2) the tunica media or middle layer containing elastic fibers, collagen fibers and smooth muscle cells, and 3) the tunica adventitia or outer layer of connective tissue. Capillaries are an exception, since they only consist of a tunica intima. The composition of elastic fibers, collagen fibers and smooth muscle cells varies throughout the vascular tree. Where arteries primarily contain elastic fibers, smooth muscle cells are predominant in arterioles, and collagen fibers in the vena cava.[12,30] These differences in vessel wall structure explain the unique function of each blood vessel type.

Figure 6, shows the pressure-volume curve of a typical artery (red curve) and vein (blue curve). An index of vessel expansibility is elasticity *(E)*, which is the slope of the tangent to any point along the pressure-volume *(P-V)* curve (Equation 9).[9,12,30]

$$E = \frac{\Delta P}{\Delta V} \tag{9}$$

As the blood vessel wall is heterogeneous tissue, elasticity varies depending on the volume inside the vessel. In the beginning, the pressure-volume curve of both the artery and vein is relatively flat (low elasticity); a certain volume increase *(ΔV)* leads only to a small pressure increase *(ΔP)*. However, the slope (and thus elasticity) increases as the volume increases. Due to vessel stiffening a similar volume increase *(ΔV)* now leads to a larger pressure increase *(ΔP↑)*. The pressure-volume relation is certainly not linear, but curvilinear; pressure increases more rapidly as volume increases.[12,30] Comparison of both pressure-volume curves shows that, in the high pressure range (arterial system (red)), elasticity of the arteries is high due to the elastic fibers. In contrast, in the low pressure range (venous system (blue)) elasticity of the veins is low due to the smooth muscle cells and collagen fibers. The high elasticity of arteries allow the aorta and arteries to act as reservoirs of elastic energy that buffer the pulsatile heart outflow.[3,10,30] While, the low elasticity of veins allow the venous system to act as a volume reservoir.[10] However, for the high pressure range, elasticity of the veins becomes quite similar to that of arteries, making veins suitable for use as arterial bypass grafts.[12]
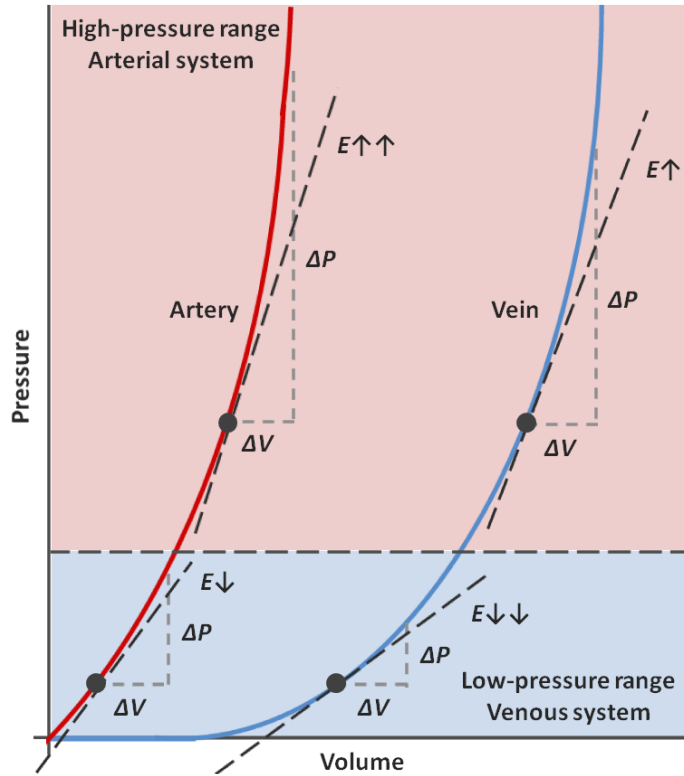
Figure 6. Representation of the relation between pressure and volume of a typical artery (red curve) and vein (blue curve). Elasticity is the slope of the tangent to any point along the curve.

IMPLEMENTATION OF THE VASCULAR TREE OF BLOOD VESSELS INTO THE MODEL

The vascular blood vessel tree of this cardiovascular model is simplified into a concatenation of straight hollow tubes containing five levels of arborisation, namely aorta (1x), large arteries (1x intra- and 1x extracranial), small arteries (2x intra- and 2x extracranial), arterioles (2x intra- and 2x extracranial), and the microcirculation & venous system (1x), see figure 3.

Different methods can be used to model blood flow through the vascular tree of blood vessels. For simplicity, first assume a constant and nonpulsatile blood flow throughout the circulatory system.

OHM'S LAW OF HYDRODYNAMICS

For this situation it is allowed to apply the classical hydrodynamic laws, of which the most important one is analogous to Ohm's law of electricity.[10,12] For electricity, the potential difference *(ΔV)* across two points equals the product of current *(I)* and resistance *(R)*, while for liquids, the pressure difference *(ΔP)* between an upstream and downstream point equals the product of flow *(Q)* and resistance *(R)* between these points (Equation 10).[7,10,12,19,21]

$$\Delta V = I \cdot R \qquad for\ electricity$$
$$\Delta P = Q \cdot R \qquad for\ liquids$$

(10)

Rearrangement of equation 10 shows that flow *(Q)* can be described as the difference in pressure *(ΔP)* divided by the resistance *(R)* (Equation 11).

$$Q = \frac{\Delta P}{R}$$

(11)

Ohm's law of hydrodynamics holds at any instance in time, regardless how simple or complex the circulatory system. In addition, this law is geometry independent as it requires no assumptions about whether vessels are compliant or rigid as long as the resistance in the vessel remains constant.[12]

THE POISEUILLE-HAGEN EQUATION

In case of a constant and nonpulsatile blood flow throughout the circulatory system, it is also allowed to apply the Poiseuille-Hagen equation, which determines flow *(Q)* based on vessel geometry (vessel radius *(r)* and length *(l)*) and fluid properties (blood viscosity *(η)*) (Equation 12).[12,15]

$$Q = \Delta P \cdot \frac{\pi \cdot r^4}{8 \cdot \eta \cdot l} \tag{12}$$

In contrast to Ohm's law, the Poiseuille-Hagen equation requires the following assumptions:[3,12,15]

1. Fluid must be incompressible
2. Fluid viscosity must be constant
3. Each blood vessel must be straight, rigid, cylindrical and unbranched, and have a constant radius
4. Fluid velocity must be zero near the vessel wall (no slip condition)
5. Flow must be steady and nonpulsatile
6. Flow must be laminar

The first five conditions are well met by our model as blood can be considered as an incompressible fluid (first condition), showing no 'slippage' (fourth condition). Due to the high pressures found in the arterial system, whole blood acts like a non-Newtonian fluid with a constant viscosity (second condition). In addition, our vascular tree of blood vessels is simplified into a concatenation of straight rigid hollow tubes (third condition). Although our vascular tree contains branches and vessels vary in radius, each individual vessel at a particular level of arborisation is unbranched and has a constant radius.[12] Furthermore, for simplicity we assumed a constant and nonpulsatile flow throughout the circulatory system (fifth condition). However, it is unclear whether our model fulfils the last prescribed condition. Blood flow is indeed laminar in cylindrical vessels up to a certain point. Ohm's law of hydrodynamics states that flow increases linearly with pressure difference, if resistance remains constant (Equation 11). However, beyond a critical value of the dimensionless Reynolds number *(Re)* (Equation 13), resistance increases instead of remaining constant, making flow no longer proportional to pressure difference, but to approximately the square root of *ΔP*, see figure 7.

$$Re = \frac{2 \cdot r \cdot v \cdot \rho}{\eta} \tag{13}$$

$v = velocity\ of\ blood\ flow$
$\rho = density\ of\ blood$

Blood flow is laminar when *Re* is below approximately 2000, while it is mostly turbulent when *Re* exceeds 3000.[12] In healthy situations *Re* does normally not exceed 3000. However, turbulent flow may appear in the aorta, due to its large radius.[12]
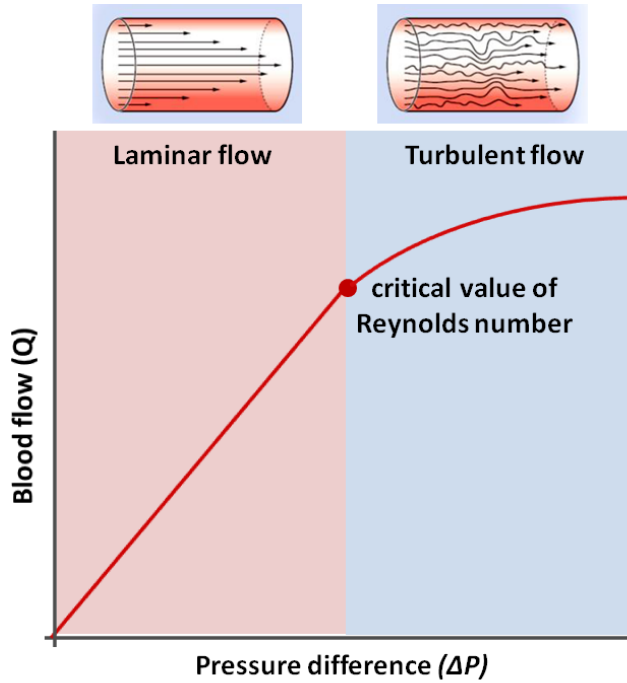
Figure 7. Representation of the relation between blood flow and pressure difference. Below the critical value of Reynolds number, blood flow is laminar, while above it is turbulent. Adapted from Medical Physiology (Boron and Boulpaep).[12]

In conclusion, it seems that both Ohm's law and the Poiseuille-Hagen equation are applicable for a nonpulsatile circulatory system of rigid straight cylindrical vessels. If we reconsider our simplification, it turns out that in reality flow cannot be nonpulsatile, as the heart is a pump with an ejection and filling phase resulting in a pulsatile flow.[3,12] This makes that Ohm's law is used to model blood flow in our cardiovascular system instead of the Poiseuille-Hagen equation which assumes a nonpulsatile flow.

Furthermore, it is too simplistic to consider the vascular blood vessel tree as a concatenation of resistors *(R)* and thus to ignore the elastic properties of the blood vessels. In order to implement these elastic properties, the famous two-element Windkessel model is used. Now, instead of modelling each vessel segment by a single resistor, a parallel capacitor *(C)* is added describing the elastic and storage properties of the vessel, see figure 8.[2,9,10] The Windkessel effect attenuates the pulsatile blood flow to deliver it more continuously to the organs and tissues.[30]
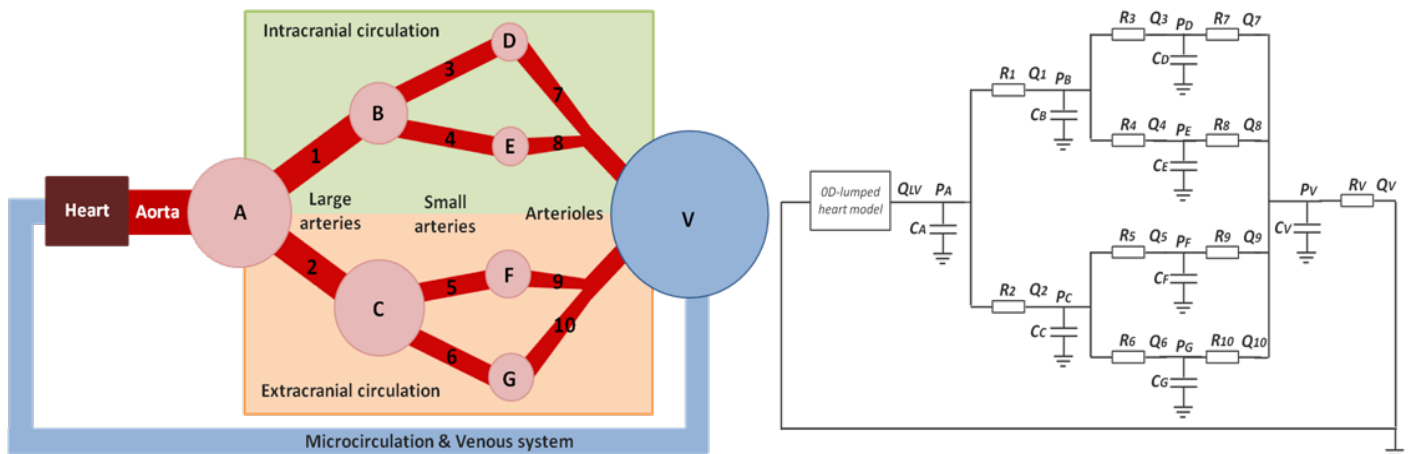

Figure 8. Vascular tree of cardiovascular model. On the left: two-element Windkessel model. On the right: electrical equivalent. Q = blood flow, P = pressure, C = capacitance and R = resistance.

Just as the resistor describes the linear relation (at least below the critical Reynolds number) between pressure difference and flow, the capacitor describes the relation between pressure *(P)* and volume *(V)*. The pressure-volume curve is strongly related to the ability of blood vessels to expand and is certainly not linear as seen in

figure 6. Though, it is not clear whether the pressure-volume curve is best described by an exponential[10,22] or quadratic function. In this cardiovascular model we have chosen for the exponential function given by equation 14, assuming a pressure of 0 mmHg when the compartment is completely empty (V = 0 mL).

$$P = \left(exp\left(\frac{V}{C}\right)\right) - 1 \tag{14}$$

$C = capacitance$

This choice is based upon the fact that in literature also a nonlinear relation between elasticity and pressure is described,[30] while this would be linear in case of a quadratic function.

By using both equations 11 and 14, pulsatile flow is modelled through the vascular tree of blood vessels. Each vessel compartment has a fixed capacitance and contains a certain amount of volume at any moment in time. Based on these two parameters the corresponding pressure in each vessel compartment is determined (Equation 14), making it possible to compute the pressure difference between consecutive vessel compartments. By knowing the resistance over each vessel segment, blood flow in each vessel segment is determined by means of equation 11. It is assumed that backflow of blood is impossible, as fluids generally only flow from a higher to a lower pressure, and pressure decreases along the vascular tree.[12] From the large arteries (parent compartment A) blood can flow into two small arteries (child compartments B and C). The same holds for flow from small arteries (parent compartments B and C) into arterioles (child compartments D to G). On arteriolar level, outflow of each of the four arterioles (compartments D to G) is merged and pumped into the microcirculation & venous compartment (V). The principle of continuity of flow states that the flow in each level of arborisation should be equal over the total heart period.[10,12,15]

PARAMETER CHOICE - VASCULAR TREE OF BLOOD VESSELS

According to Ohm's law of hydrodynamics (Equation 10), resistance *(R)* equals pressure difference *(ΔP)* divided by flow *(Q)* (Equation 15).[7,10,12,19,21]

$$R = \frac{\Delta P}{Q} \tag{15}$$

When we apply this equation to the entire systemic circulation, total peripheral resistance (TPR) equals the difference in mean arterial pressure (MAP) and mean venous pressure (MVP) divided by the CO, with TPR being the sum of the resistances of all vascular structures within the systemic circulation.[9,12,18] The arterial blood pressure in the large systemic arteries varies between the systolic pressure (P_{sys} ≈ 120 mmHg) and the diastolic pressure (P_{dias} ≈ 80 mmHg), leading to the following MAP (Equation 16).[12]

$$\mathrm{MAP} \approx P_{dias} + \frac{1}{3}\left(P_{sys} - P_{dias}\right) \approx 93.3 \; mmHg \tag{16}$$

MVP or central venous pressure corresponds to the pressure in the right atrium, which is normally around 3 mmHg.[12,18] This leads to the following TRP (Equation 17).

$$\mathrm{TPR} = \frac{\mathrm{MAP-MVP}}{\mathrm{CO}} = \frac{93.3-3}{87.5} = 1.03 \; \frac{mmHg}{mL/s}\,(PRU) = 1376.5\frac{dyne \cdot s}{cm^5} = 1376.5 \cdot 10^5 \frac{kg}{s \cdot m^4} \tag{17}$$

In our cardiovascular model TPR is made up from multiple resistors in series, namely the different levels of arborisation: large arteries, small arteries, arterioles, and microcirculation & venous system. Besides, each level of arborisation contains parallel intracranial and extracranial vessels (Equation 18).

$$\mathrm{TPR} = \underbrace{\frac{1}{\frac{1}{R_1}+\frac{1}{R_2}}}_{R_{large\;arteries}} + \underbrace{\frac{1}{\frac{1}{R_3}+\frac{1}{R_4}+\frac{1}{R_5}+\frac{1}{R_6}}}_{R_{small\;arteries}} + \underbrace{\frac{1}{\frac{1}{R_7}+\frac{1}{R_8}+\frac{1}{R_9}+\frac{1}{R_{10}}}}_{R_{arterioles}} + R_v \tag{18}$$

Figure 9 represent the pressure profile along the systemic circulation. It shows that the steepest pressure drop (from 85 to 25 mmHg) occurs in the arterioles. In agreement with the principle of continuity of flow and equation 15, this means the greatest vascular resistance is found in the arterioles. As much as 65% of the TRP is defined by the arterioles. In addition, the pressure drop in the arteries is from 93.3 to 85 mmHg (~10%): from 93.3 to 90 mmHg in the large arteries and from 90 to 85 mmHg in the small arteries. Furthermore the capillaries also account for approximately 10% (from 25 to 15 mmHg) and the venous system for approximately 15% (from 15 to 3 mmHg).[4,12]
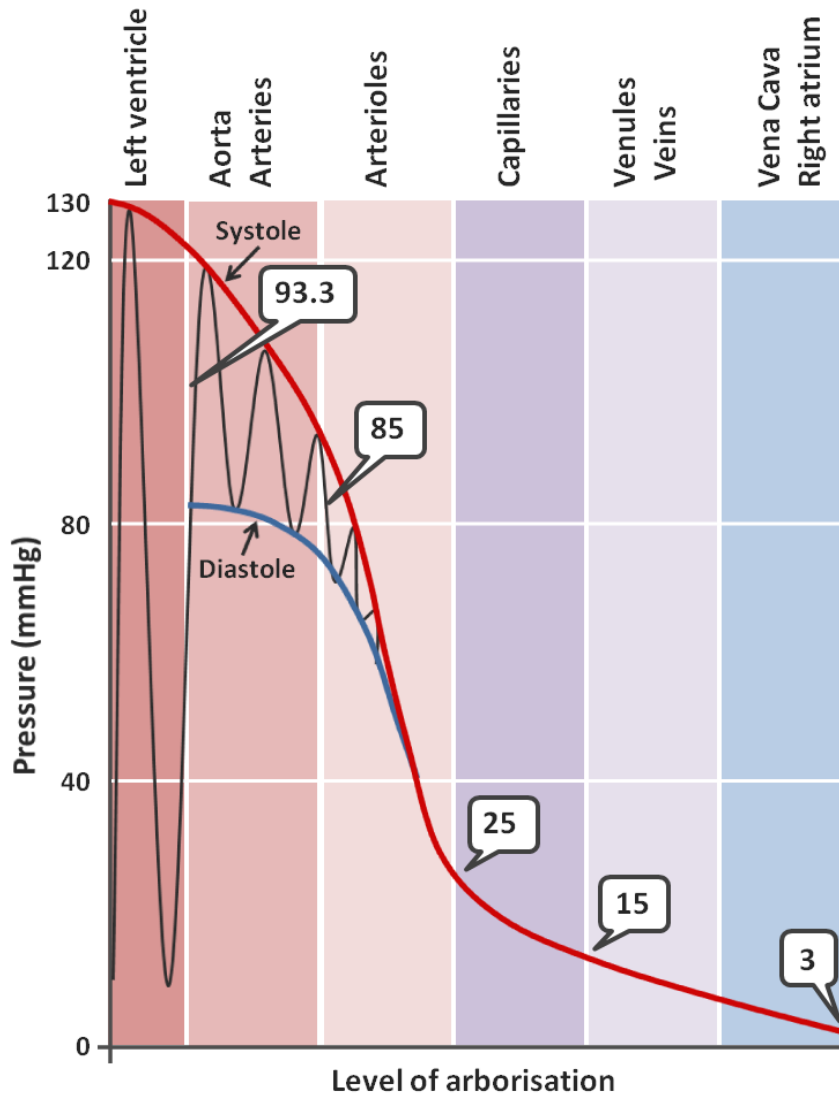

Figure 9. Pressure profile along the systemic circulation. Adapted from Medical Physiology (Boron and Boulpaep).[12]

In addition, it is known that the intracranial circulation receives 15% of the resting CO, while the remaining 85% flows through the extracranial circulation.[12,18,27] This makes it possible to calculate the resistance over each individual vessel segment, see table 4. This relatively large supply of blood is needed to accomplish the huge demand for O_2 and nutrients of the brain. Of all body organs, the brain is the least tolerant for a disturbance in blood supply. An interruption in cerebral blood flow of just a few seconds can cause unconsciousness, while after a few minutes irreversible cellular damage of neurons is likely.[12,27,31]

Table 4. Resistance, pressure and flow values for each vessel segment of the cardiovascular model. I = intracranial vessel, E = extracranial vessel.

	Resistance (kg/(m⁴·s)	Pressure (mmHg)	Pressure (Pa)	Flow (mL/s)
Large arteries	5079365	93.3	12438.9	87.5
1 (I)	33862434	93.3		13.1 (15%)
2 (E)	5975724	93.3		74.4 (85%)
Small arteries	7619048	90.0	11999.0	87.5
3 (I)	101587302	90.0		6.6 (7.5%)
4 (I)	101587302	90.0		6.6 (7.5%)
5 (E)	17927171	90.0		37.2 (42.5%)
6 (E)	17927171	90.0		37.2 (42.5%)
Arterioles	91428571	85.0	11332.4	87.5
7 (I)	1219047619	85.0		6.6 (7.5%)
8 (I)	1219047619	85.0		6.6 (7.5%)
9 (E)	215126050	85.0		37.2 (42.5%)
10 (E)	215126050	85.0		37.2 (42.5%)
Microcirculation & Venous system	26462084 (diastole) ∞ (systole)	25.0	3333.0	87.5
Heart		3.0	400.0	87.5

According to equation 14, capacitance depends on the average pressure (table 4) and volume (table 2) of each compartment. Table 5 summarizes the corresponding capacitance of each vessel compartment.

Table 5. Volume, pressure and capacitance values for each vessel compartment of the cardiovascular model. I = intra-cranial vessel, E = extracranial vessel.

	Volume (mL)	Pressure (mmHg)	Capacitance·10⁻⁹ (L/Pa)
Large arteries	300	93.3	31816.4
A	300	93.3	31816.4
Small arteries	300	90.0	31939.8
B (I)	12	90.0	1277.6
C (E)	288	90.0	30662.0
Arterioles	150	85.0	16067.7
D (I)	3	85.0	321.4
E (I)	3	85.0	321.4
F (E)	72	85.0	7712.4
G (E)	72	85.0	7712.4
Microcirculation & Venous system	3500	25.0	431460.0
Heart	120	3.0	

COUPLING OF HEART COMPARTMENT TO VASCULAR TREE OF BLOOD VESSELS

Coupling of the 0D lumped model of the heart compartment to the 1D distributed model of the vascular blood vessel tree, gives us the opportunity to model blood flow through the cardiovascular system, with as focus areas the systemic and intracranial circulation.

This is done, by presuming a volume driven system. The complexity of the model combined with the intention to simulate in real-time, makes it impossible to model the blood flow continuously. However, according to equation 2, flow equals an amount of volume per unit of time, making it a concatenation of (small) volume quanta. The amount of blood volume flowing out of the heart and via the aorta into the large arteries each time unit, depends on the sampling interval *(Δt)*. The same holds for the vascular vessel tree; as a result of

generated flow, a certain amount of blood flows each time unit out of the parent compartment and into the child compartment(s). However, according to the principle of continuity of mass, the amount of volume flowing out of each compartment cannot exceed the volume present in that compartment. Total circulating blood volume remains constant, as long as no blood is added or lost.[10,12,15] In case the total amount of volume flowing out of the parent compartment exceeds the available volume, the latter is distributed in proportion over the child compartments.

At the beginning of the sampling interval each compartment (heart and blood vessels) contains a certain amount of volume (baseline). During the sampling interval there may be volume flowing into *(+ΔV)* and/or out *(-ΔV)* of each compartment. In this model it is chosen to add and subtract these volumes from the baseline volume at the very end of the sampling interval. Another option is to already add the volume flowing into the compartment to the baseline volume, and to use this new volume to calculate the volume flowing out of the compartment. The latter situation assumes that inflow and outflow of volume is instantaneous, while it takes some time *(Δt)* in our model.

In order to calculate the volume flowing into *(+ΔV)* and/or out *(-ΔV)* of each compartment, it is needed to solve the ordinary differential equation 2. In first instance the Euler method was used, which is a first-order numerical procedure for solving ordinary differential equations with a given initial condition.[32] In this case:

$$\dot{V}(t) = f(t, V) \qquad with\ as\ inital\ condition\ V(t_o) = V_o \tag{19}$$

By choosing a value *h* for the size of each sampling interval and assuming $t_n=t_0+n\cdot h$, the Euler method approximates the next value in time by the present value *(V_n)* added to an increment corresponding to the product of interval size *(h)* and estimated interval slope.[32]

$$\begin{aligned} t_{n+1} &= t_n + h \\ V_{n+1} &= V_n + h \cdot f(t_n, V_n) \end{aligned} \tag{20}$$

Estimation accuracy depends on step size *h*, where accuracy decreases as *h* increases. By being a first order method, the local error (error per step) is proportional to the square of the step size *(h²)*, while the global error (total accumulated error) is proportional to the step size *(h)*.[32] In case the error becomes too large, for example fast fluctuations (oscillations) appear. Due to the fact that the intracranial circulation is characterised by a relatively high flow (15% of total) through blood vessels containing relatively small amounts of volume (4% of total), at this location decreased estimation accuracy first leads to oscillations. Figure 10 (above) shows the intracranial blood flow curve of the small arteries (vessel segment 4). For a step size of 1 (blue curve) and 2 ms (red curve), blood flow is still accurately estimated by the Euler method. However when this interval increases to 4 ms (green curve), the flow curve shows large fluctuations around the curve seen at 1 and 2 ms.

To improve estimation accuracy, higher-order techniques such as Runge-Kutta methods or linear multistep methods are needed.[32] In this cardiovascular model we have chosen to extend the Euler method, which is actually a first-order Runge-Kutta method, into the famous fourth-order Runge-Kutta method. The latter is commonly referred to as "classical Runge-Kutta method" or "the Runge-Kutta method". For the same ordinary differential equation and initial condition (Equation 19), step size *h* and assumption $t_n=t_0+n\cdot h$, the Runge-Kutta method approximates the next value in time by the present value *(V_n)* plus a weighted average of four increments *(k_1 to k_4)*, where greater weight is given to increments at the midpoint of the interval *(k_2 en k_3)*.[32]

$$\begin{aligned} t_{n+1} &= t_n + h \\ V_{n+1} &= V_n + \frac{1}{6}h(k_1 + 2k_2 + 2k_3 + k_4) \qquad with\ \ k_1 = f(t_n, V_n) \\ & \hspace{6.5cm} k_2 = f(t_n + \frac{h}{2}, V_n + \frac{h}{2}k_1) \\ & \hspace{6.5cm} k_3 = f(t_n + \frac{h}{2}, V_n + \frac{h}{2}k_2) \\ & \hspace{6.5cm} k_4 = f(t_n + h, V_n + hk_3) \end{aligned} \tag{21}$$

By not only taking into account the slope *(k₁)* at the beginning of the interval (the Euler method), but also the slope at the midpoint *(k₂ and k₃)* and at the end of the interval *(k₄)*, a more accurate estimation is obtained in comparison to Euler. For fourth-order methods, local error is proportional to the fifth power of step size *(h⁵)*, while global error is proportional to the fourth power of step size *(h⁴)*.[32] Figure 10 (below) shows the intracranial blood flow curve in the small arteries obtained by the Runge-Kutta method. Comparison of both methods shows, that for small step sizes (1 and 2 ms) still similar results are obtained. However, for a step size of 4 ms still quite reliable results are obtained by the Runge-Kutta method, while at 8 ms the blood flow curve shows oscillations. Nevertheless, these oscillations are not as prominent as for the Euler method, due to a local and global error reduction proportional to the third power of step size *(h³)*.[32]
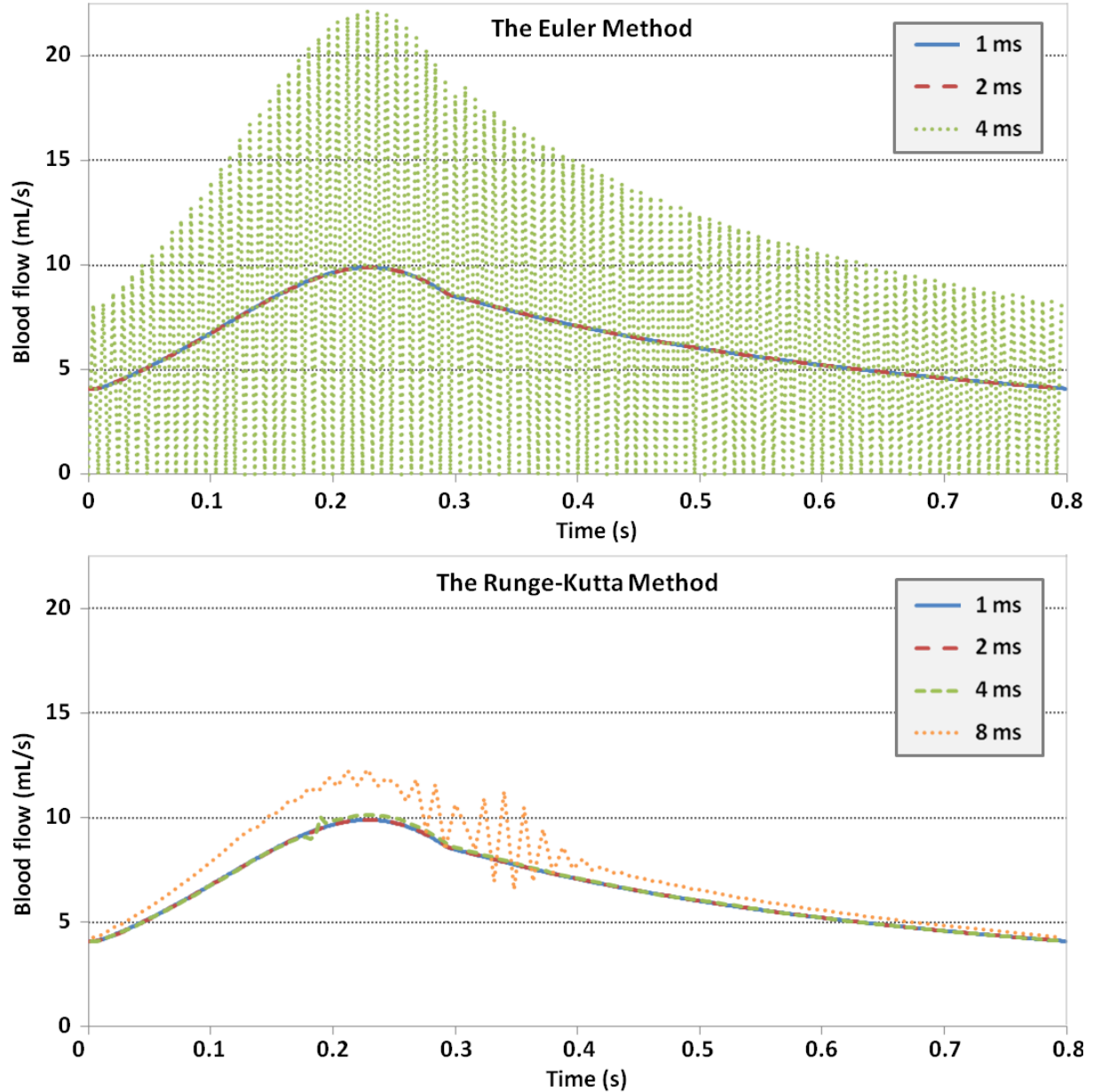

Figure 10. Intracranial blood flow curve in small arteries (vessel segment 4) for different step sizes. Above: estimation by the Euler method; below: estimation by the Runge-Kutta method.

For real-time simulation, a default sampling interval of 1 ms (0.001 s) is implemented, corresponding to a sampling frequency of 1000 Hz. Normally, this should be long enough to execute all computations. However, in case of a slow calculation system, sampling interval can be manually increased to 2 ms to maintain real-time simulation. According to figure 10, higher values are undesirable as oscillations hamper proper simulations.

THE ARTERIAL ACCELERATION

At this moment, all the energy needed to distribute and transport blood through the entire circulatory system is delivered by a single energy source, namely the heart.[1,12] The blood flow curve of figure 10 contains one peak during the systolic phase, originating from the pulsatile pressure and flow waves generated by the active heart contraction. However, during the majority of TCD measurements two systolic peaks are observered.[33] In general, it is assumed that the second systolic peak is the result of wave reflections. At transitions in vessel geometry (e.g. bifurcations, stenoses or aneurysms)[1,34] or properties (e.g. stiffness, resistance or radius),[1] the forward travelling wave is partly reflected, causing a backward travelling wave to the heart. Consequently, pressure and flow waves can be seen as a superposition of a forward travelling wave and (several) backward travelling wave(s).[1,34] The position of the second systolic peak mainly depends on the arterial stiffness.[1,34,35] Due to the low arterial stiffness seen in young individuals, the pulsatile pressure and flow waves are attenuated (Windkessel effect) and wave velocity is relatively low. This results in reflected waves, with rather small amplitudes, arriving during the late systole or early diastole. In contrast, arterial stiffening of blood vessels seen in elderly, results in reflection waves with larger amplitudes (less damping of pulsatile wave), arriving during the early systole (high wave velocity).[1] In addition, location of the second peak can be influenced by the CO, HR, blood pressure and location of blood vessel in the arterial tree.[34,35]

Due to the fact that we assume no backflow of blood in this cardiovascular model, wave reflections cannot emerge and no second systolic peak exists. This means that we need to adapt our assumption in order to model wave reflections. Before doing this, let us first further investigate the two systolic peaks seen in the majority of TCD measurements of the MCA. Clinical data obtained over a wide variety of individuals and physiological situations, demonstrates that both peaks show different behaviour. The sys1 component remains quite constant over different physiological conditions, while the sys2 component varies a lot with the HR, CO and CO_2 level.[36] These differences in behaviour indicate a different origin of both systolic peaks. In our opinion it is questionable whether the heart contraction and corresponding wave reflections are responsible for the occurrence of these two peaks. As both phenomena are influenced by the HR, CO[34,35] and CO_2 level, we would expect both peaks to vary during different physiological conditions. We cannot explain the observation of a sys1 component that remains quite constant. In our opinion it is furthermore questionable whether the heart alone is capable of delivering all the energy needed for blood distribution over the entire circulation system. As mentioned earlier the cross sectional area of the arterial system increases dramatically from aorta towards peripheral capillaries (table 3).[12] As a result the pressure wave is distributed over an immense area. Theoretically this will lead to a weaker pressure wave, nevertheless the opposite is seen. The propagation of the pressure wave increases on its way from aorta to peripheral capillaries.[18] A similar situation is seen for the difference between systole and diastole (pulsatility). Logically this difference decreases in a widely expanding arterial vessel tree, due to an expected decrease in pressure wave strength. However, pulsatility also increases further away from the heart.[18] So both conducting speed of the pressure wave as well as pulsatility increases towards periphery. In our opinion, this is impossible in case the heart is the only energy source for pressure wave distribution. As backward travelling waves are counteracting propagation of the forward travelling wave, it seems not logical that wave reflections are responsible for the occurrence of a second systolic peak.

Our hypothesis is that the sys1 component originates from a brief and rapid active contraction (myogenic response) of the conducting arteries to support the propagation of the pressure wave from the heart towards peripheral capillaries. While the sys2 component originates from the active contraction of the heart itself.[36] This hypothesis is based on the assumption that there must be another source adding energy to the pressure wave originating from the heart, to increase conducting speed and pulsatility. We assume that this energy is delivered by the conducting arteries on a beat-to-beat basis, through active contraction of vascular smooth muscle cells (VSMCs) in the arterial vessel wall. Since VSMCs are sensitive for fast changes in pressure, a sudden increase in pressure will stretch the VSMCs and cause vasoconstriction of the blood vessel, whereas a sudden decrease in pressure leads to vasodilatation.[12] During each heart contraction, pressure increases rapidly at the

beginning of the arterial tree, reaching some minimum stretch threshold. This provokes a local myogenic response through vasoconstriction of that specific vessel part. The myogenic response will spread over the entire arterial vessel tree like a peristaltic movement. Active contraction of VSMCs at the beginning of the arterial tree will induce a rapid increase in pressure and thus a myogenic response in the consecutive part of the vessel tree and so on. In this way the myogenic response can rapidly spread over the entire arterial tree of blood vessels, resulting in the increased propagation speed of the pressure wave from heart towards periphery.[37] Furthermore, our hypothesis makes it easier to understand the differences in behaviour of both systolic peaks. Since the sys1 component is caused by the myogenic response, it depends on the timing and spreading of the response. Once the myogenic response is provoked, it follows a constant pattern, resulting in a sys1 component that remains quite constant over a variety of physiological conditions. The sys2 component is caused by the heart contraction and thus depends on CO, HR, ABP and peripheral vessel resistance. It is therefore logical that the sys2 component varies for changes in these parameters.

IMPLEMENTATION OF THE ARTERIAL ACCELERATION INTO THE MODEL

Since the vascular blood vessel tree of this cardiovascular model only contains five levels of arborisation, it is impossible to implement the peristaltic-like movement of the myogenic response. Contraction of the large arteries all at once, leads to such a fast increase in pressure that the blood flow curve starts to oscillate as huge amounts of blood suddenly flow into the small arteries. Therefore, we have chosen to provoke an equal myogenic response in all consecutive arterial blood vessels at the same time. Commonly, the myogenic response is initiated in the large arteries, as the pressure wave from the heart first arrives in these vessels. In this situation not only a myogenic response is provoked in the large arteries but simultaneously in the small arteries and arterioles. However, occasionally the myogenic response is initiated in the small intracranial (or extracranial) vessels, thereby provoking a response in the intracranial (or extracranial) small arteries and arterioles only. During this heart period it is impossible to provoke another myogenic response in the large arteries, because peristalsis is only directed forwards.

To initiate a myogenic response, arterial blood vessel compartments (A, B and C) must meet four conditions:
1. Pressure change over time *(dP/dt)* must exceed the minimum stretch threshold.
2. Pressure inside the vessel compartment must exceed 50% of the default pressure (table 4 and 5); VSMCs in the arterial vessel wall should be under some tension, otherwise they cannot be stretched.
3. The myogenic response should be initiated during the first third of systole. The sys1 component appears during the systolic upstroke and precedes the sys2 component originating from heart contraction. Total duration of systole is about 300 ms, wherein systolic upstroke takes approximately the first 100 ms.[12,33,36]
4. A myogenic response can only be provoked once during a heart period.

In case all prescribed conditions are met, myogenic response is modelled by changing the fixed default vessel compartment capacitance *(C$_{default}$)* by the following sinusoidal function:

$$C = C_{default} - \frac{sin\,(x) \cdot S_{MR}}{100} \cdot C_{default} \qquad with\ x = \left(\frac{t}{T}\right) \cdot \pi \qquad\qquad (22)$$

$t = time$
$T = duration\ of\ myogenic\ response$
$S_{MR} = strenght\ of\ myogenic\ response$

The strength of the myogenic response is equal for all vessel compartments, creating an equal percentage decrease of capacitance. However, due to the exponential relationship between pressure and volume (Equation 14), a similar percentage decrease in capacitance will lead to a larger pressure increase in case of a high baseline pressure (large arteries), and to a smaller pressure increase in case of a low baseline pressure (arterioles). As a result, the pressure difference between consecutive vessel compartments increases more at the beginning of the arterial vessel tree and less at the end. Since resistance remains constant, flow increases more in the large arteries and less in the arterioles. Just as the pressure wave generated by heart contraction

weakens on its way through the circulatory system, the myogenic response is less prominent at the end of the arterial system. This phenomenon can be explained by the fact that the amount of VSMCs decline along the arterial system.[38]

PARAMETER CHOICE - THE MYOGENIC RESPONSE

Elasticity is an index of vessel expansibility and thus indicates the amount of stretch in a certain blood vessel. As the VSMCs are sensitive for fast changes in pressure, the minimum stretch threshold is defined as the minimum amount of 'stretch' in pressure needed to provoke a myogenic response. The minimum stretch threshold (ST_{MR}) of each arterial vessel compartments is therefore defined as the product of elasticity (E) and pressure (P) in the compartment at the systolic onset (Equation 23).

$$ST_{MR} = E \cdot P \qquad with\ E = \frac{\Delta P}{\Delta V} \qquad\qquad (23)$$

This stretch threshold is the highest in the large arteries (150 mmHg²/mL), due to the high elasticity and pressure found in the large arteries compared to the small arteries. Furthermore, it is higher in the extracranial small arteries (145 mmHg²/mL) compared to the intracranial small arteries (140 mmHg²/mL). This difference can be explained by the fact that 15% of the CO flows through only 4% of the total amount of blood vessels each heart period. This creates relatively larger fluctuations in volume and thus pressure during the heart period, making the end-diastolic pressure and elasticity lower in the intracranial circulation compared to extracranial.

Normally the sys1 component originates from a concatenation of myogenic responses rapidly spreading over the entire arterial blood vessel tree. However, in this cardiovascular model the combined effect of all these individual responses is provoked by just one overall myogenic response. As the final shape of the sys1 component depends on the duration and strength of this overall myogenic response, we used TCD measurements of healthy individuals to estimate both parameters. Comparable results were obtained when the myogenic response lasted 120 ms and had strength 5, see figure 11. This strength corresponds to a maximal decrease in capacitance of 5%.
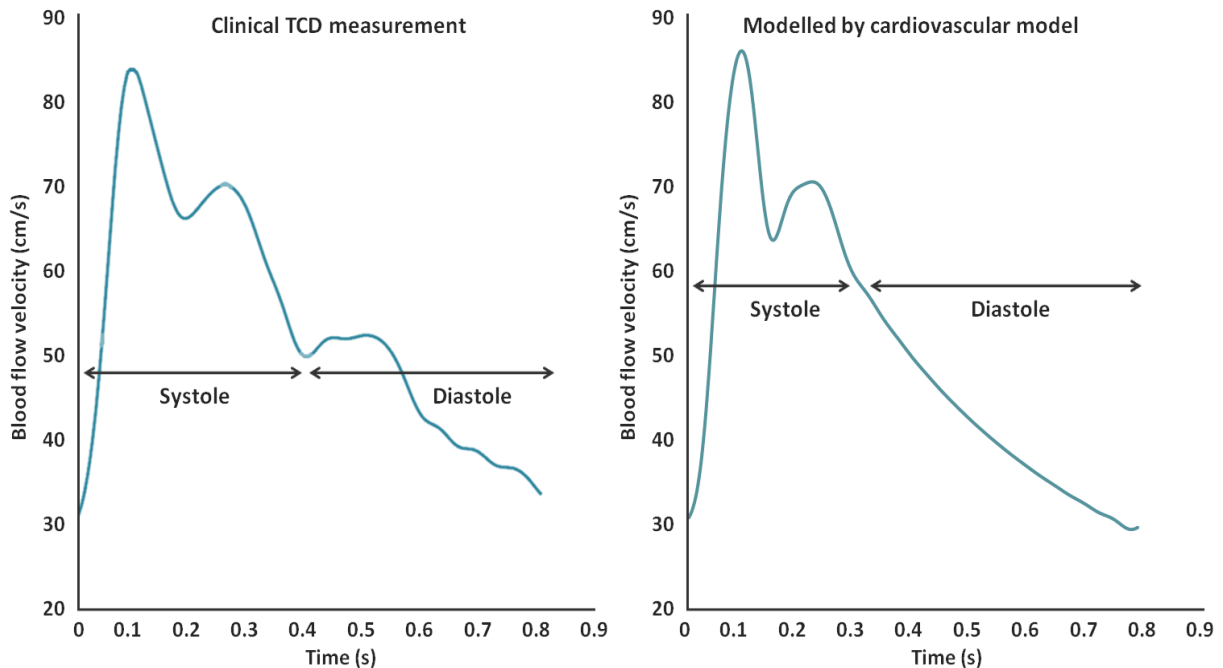

Figure 11. Blood flow velocity measured in healthy individuals (left) and modelled by the cardiovascular model (right).

Table 6. Initial parameter conditions - myogenic response.

Parameter	Initial condition	Remarks
Stretch threshold large arteries	150 mmHg^2/mL	
Stretch threshold intracranial small arteries	140 mmHg^2/mL	
Stretch threshold extracranial arterioles	145 mmHg^2/mL	
Duration of myogenic response	120 ms	
Strength of myogenic response	5	5% decrease of capacitance

RESPONSES

This cardiovascular model aims to provide insight into intracranial hemodynamics. At this moment intracranial blood flow increases linearly with an increase in pressure difference, according to Ohm's law of hydrodynamics (Equation 11). As a result, intracranial blood flow is strongly affected by changes in for example CO, HR or ABP. However, in reality cerebral blood flow averages 50 ml/min for each 100 grams of brain tissue[12,39] and remains relatively stable (between 50 and 55 ml/100g/min) over a variety of physiological conditions.[40] Several mechanisms are responsible for the regulation of both intra- and extracranial blood flow. We have chosen to implement three of the most important mechanisms for blood flow regulation into this cardiovascular model: the autoregulation mechanism, the central nervous system (CNS) ischemic response and the baroreceptor response.

THE AUTOREGULATION MECHANISM

Optimal functioning of organs and tissues largely depends on a stable supply of nutrients and removal of waste products, making them very sensitive for changes in blood flow.[12,41] Autoregulation is a mechanism aiming to maintain a stable and constant blood flow, despite variations in blood pressure.[31,39,40,42,43] Due to the importance of this mechanism, autoregulation can be found in many circulatory systems, like in the coronary, cerebral and renal circulation. In particular, it is well developed in the human cerebral circulation, since of all organs and tissues the brain is the least tolerant for a disturbance in blood supply.[12,39]

Autoregulation is especially a local phenomenon which can be initiated by neurogenic, myogenic or metabolic control mechanisms.[12,39,40] However, most clinical evidence is found for an important active role of the metabolic control mechanism.[39] Due to changes in brain metabolism, oxygenation or blood flow, locally metabolites accumulate or dissipate in the brain, like O_2, CO_2, hydrogen, potassium, calcium or adenosine.[39,40] Especially the autoregulatory effect of changes in arterial partial pressure of CO_2 *(P_aCO_2)* is well known: hypercapnia causes vasodilatation of cerebral arterioles to increase cerebral blood flow, whereas hypocapnia causes vasoconstriction to decrease flow, see figure 12 (light blue dashed curve). At a normal P_aCO_2 of 5.3 kPa, blood flow equals the average value of 50 mL/100g/min. However, at a P_aCO_2 of 10.6 kPa, cerebral blood flow is twice as large as normal (100 mL/100g/min), while reducing P_aCO_2 to 2.7 kPa leads to halving of the normal blood flow (25 mL/100g/min).[39,40]

Despite the huge O_2 demand of the brain, the autoregulatory effect of changes in O_2 are less dramatic compared to that of CO_2. Figure 12 (red dashed curve) shows that only marked hypoxemia, P_aO_2 below 8 kPa, causes vasodilatation of cerebral arterioles to increase blood flow. For a P_aO_2 above 8 kPa, cerebral blood flow does not change substantially.[39,40]

The autoregulation mechanism is often divided into a static and dynamic component. The static component ensures a stable cerebral blood flow despite variations in MAP, when both variables are measured in steady state (taking 30 seconds or longer).[40–42] Figure 13 shows the static autoregulation curve (red dashed curve); cerebral blood flow remains constant over a pressure range of approximately 70 to 150 mmHg.[12,31,39,40,42,43] The dynamic component corresponds to a temporal response promoting a fast return of the cerebral blood flow to its original value after a sudden change in MAP. This response normally lasts for 2 to 10 seconds after the disturbance.[40–42]
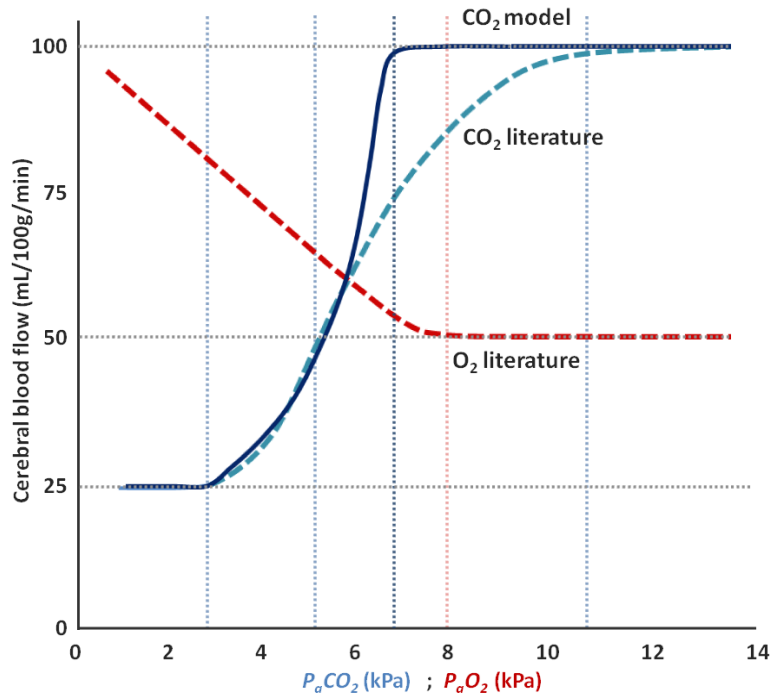
Figure 12. Relation between cerebral blood flow and P_aCO_2 - literature (light blue dashed curve) and P_aO_2 - literature (red dashed curve) and P_aCO_2 - cardiovascular model (dark blue curve). Dashed vertical lines correspond to values 2.7, 5.3, 6.7, 8 and 10.6 kPa (from left to right).
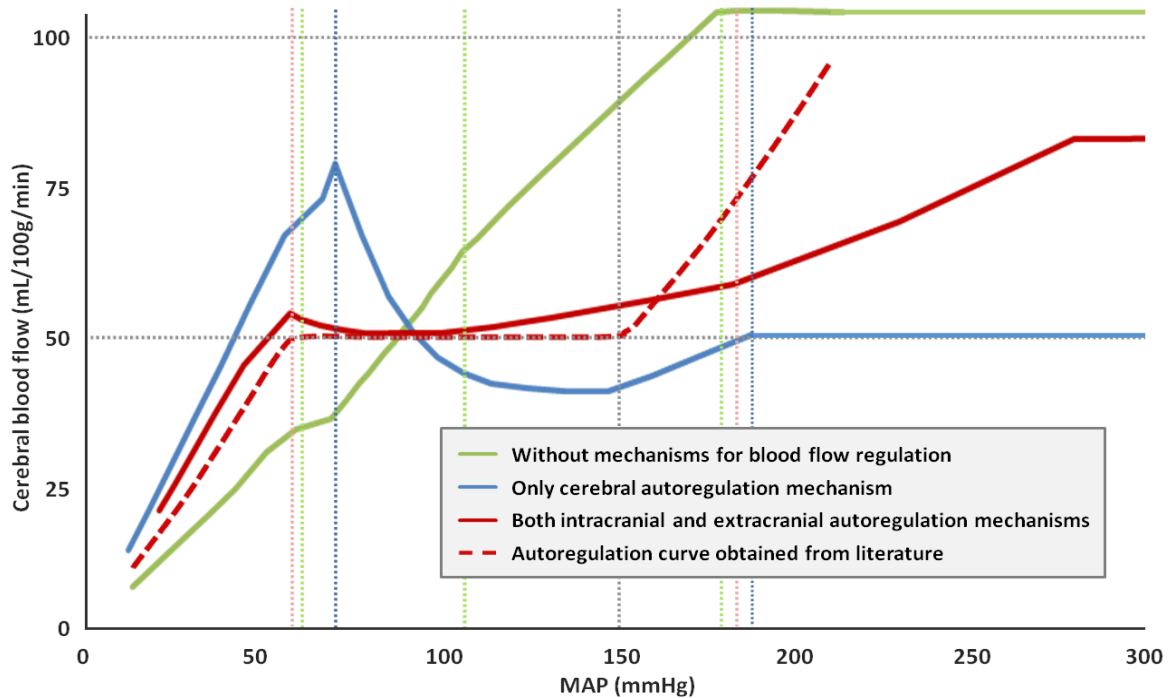

Figure 13. Static autoregulation curve obtained from literature (red dashed curve). Cerebral blood flow is kept constant between 70 and 150 mmHg. Autoregulation curves obtained by cardiovascular model; no regulation mechanisms (green curve), only intracranial autoregulation (blue curve) and both intra- and extracranial autoregulation (red curve).

IMPLEMENTATION OF THE AUTOREGULATION MECHANISM INTO THE MODEL

In this cardiovascular model, the static autoregulation component initiated by metabolic control mechanisms is implemented. We have chosen to use CO_2 as the initiator of the autoregulation response, as its effect is well described and considered to be stronger and more sensitive compared to changes in O_2 or other metabolites.[39,40] Since the autoregulation mechanism is also found outside the cerebral circulation, a similar, but less prominent, response is implemented for the extracranial circulation.

23

CO_2 is transported in the blood from the organs and tissues to the lungs. Approximately 75% of the CO_2 molecules are transported in the red blood cells, while the remaining 25% is dissolved in blood plasma.[44] Partial pressure of CO_2 *(PCO₂)* refers to the amount of CO_2 gas molecules dissolved in blood plasma. According to Henry's law, concentration of CO_2 molecules dissolved in blood plasma *([CO₂]dis)* is proportional to *PCO₂* in gas phase (Equation 24).[12] Solubility of CO_2 in blood plasma is 0.0308 mM/mmHg or 0.231 mM/kPa at 37°C.[12,44]

$$[CO_2]_{dis} = s \cdot PCO_2$$

(24)

$s = solubility\ constant$

As this cardiovascular model is a volume driven system, instead of a pressure drive system, *[CO₂]dis* in each vessel compartment is determined instead of *PCO₂*. However, since the cardiovascular model is developed for use by intensivists and other clinicians, who are familiar with *PCO₂* instead of *[CO₂]dis*, the in- and output parameters are in *PCO₂*. Each vessel compartment contains a certain amount of CO_2 molecules *(n)* dissolved in a certain amount of volume *(V)* at each moment in time. In other words, each vessel compartment has a certain *[CO₂]dis* (Equation 25).

$$[CO_2]_{dis} = \frac{n_{CO_2}}{V}$$

(25)

During a sampling interval there may be blood flowing into the (child) compartment, having a *[CO₂]dis* similar to the *[CO₂]dis* of the preceding (parent) compartment. Simultaneously, there may be blood flowing out of the compartment, having the same *[CO₂]dis* as the vessel compartment itself. As a result, CO_2 molecules are added and/or removed from the initial amount of CO_2 molecules, while at the same time blood volume is added and/or removed from the initial amount of volume. By dividing the amount of CO_2 molecules remaining after the sampling interval by the remaining volume, the new *[CO₂]dis* is determined. A normal *[CO₂]dis* of arterial blood is 1.22 mmol/L or 1.22 mM, corresponding to a *PₐCO₂* of 5.3 kPa. For venous blood this is 1.41 mM, corresponding to a *PᵥCO₂* of 6.1 kPa.[44] The difference between arterial and venous blood is due to the fact that CO_2 molecules are produced in the tissues and exhaled by the lungs. By being a waste product of tissue metabolism, CO_2 is released to capillary blood in the microcirculation.[12] Since in this cardiovascular model the microcirculation & venous system is represented by a lumped compartment, a constant amount of CO_2 molecules per time unit are added to blood flowing from arterioles into the microcirculation & venous system. Generally the production (tissue metabolism) and execution (oxygenation) of CO_2 molecules is balanced, to remain a stable arterial and venous *[CO₂]dis* in blood. In the lungs each respiratory cycle a certain percentage of CO_2 molecules is exhaled, corresponding to the amount produced by the tissues.[12] As the respiratory cycle and pulmonary circulation are disregarded in this cardiovascular model, a fixed percentage (~13%) of CO_2 molecules is removed from the, still venous, blood flowing from the heart into the large arteries.

Since autoregulation is especially a local phenomenon initiated by metabolic control mechanisms, it reacts on changes in tissue *[CO₂]dis*.[39] This venous *[CO₂]dis* is represented in the cardiovascular model, by the *[CO₂]dis* of blood flowing from intra- and extracranial arterioles into the microcirculation & venous system. Due to the pulsatile blood flow, average *[CO₂]dis* over a total heart period is used to adjust the vessel resistance of intra- en extracranial arterioles: an increased *[CO₂]dis* leads to vasodilatation of arterioles to increase blood flow, while a decreased *[CO₂]dis* leads to vasoconstriction. To obtain gradual changes in vessel resistance, average *[CO₂]dis* is taken over the last three heart periods.

PARAMETER CHOICE - THE AUTOREGULATION MECHANISM

In the end we would like to obtain an autoregulation curve like figure 13 (red dashed curve). Figure 13 (green curve), shows the cerebral pressure-flow curve obtained by our cardiovascular system without any mechanisms for blood flow regulation implemented. Below a MAP of approximately 180 mmHg, cerebral blood flow increases linearly with pressure as expected by Ohm's law of hydrodynamics (Equation 11). At 180 mmHg, SV_{LV} reaches its maximum value of 140 mL. Although blood pressure continues to rise, the heart still pumps the

maximum amount of blood each heart period. Due to the constant HR, CO cannot increase anymore (Equation 8) and thus cerebral blood flow reaches a maximum of approximately 100 mL/100g/min. Below 180 mmHg, the curve consists of three linear parts with different slopes:

- Part 1 - below 60 mmHg - is defined by a blood pressure and flow curve only containing a sys2 component. Due to the low pressure inside the vessel compartments, no myogenic response can be initiated.
- Part 2 - between 70 and 110 mmHg - is defined by a blood pressure and flow curve where the sys1 component is higher than the sys2 component. This is the normal situation seen in healthy individuals.
- Part 3 - between 110 and 180 mmHg - is defined by a blood pressure and flow curve where the sys2 component is higher than the sys1 component. Due to a large SV, the sys2 component originating from the heart contraction itself becomes more prominent.

Since cerebral blood flow, as well as extracranial blood flow, increases linearly with the MAP, we are searching for a linear relation between $[CO_2]_{dis}$ and vessel resistance. Figure 12 (light blue dashed curve) is used to estimate the boundary conditions of the cerebral autoregulation mechanism, translated to PCO_2 since this parameter is more customary for clinicians. A normal P_aCO_2 of 5.3 kPa is related to a normal P_vCO_2 of 6.1 kPa and a normal cerebral blood flow of 50 mL/100g/min. This implies that cerebral arterioles are commonly slightly constricted, since cerebral flow of 13.1 mL/s (table 4) equals 786 mL/min for 1500 grams of brain tissue or 52.4 mL/100g/min. Increasing the default resistance value (table 4) 1.07 times, results in the intended flow of 50 mL/100g/min. This normal condition defines the first point on the linear curve between P_vCO_2 and vessel resistance: a P_vCO_2 of 6.1 kPa corresponds to 1.07 times the default resistance. According to figure 12 (light blue dashed curve), cerebral blood flow is halved to 25 mL/100g/min at a P_aCO_2 of 2.7 kPa, which can be achieved by increasing the default resistance value 2.45 times. As this minimum boundary condition is reached at a P_vCO_2 of 4.35 kPa, the second point on the linear curve is defined by a P_vCO_2 of 4.35 kPa corresponding to 2.45 times the default resistance. Furthermore, cerebral blood flow is doubled to 100 mL/100g/min at a P_aCO_2 of 10.6 kPa, which can be achieved by decreasing the default resistance value 0.376 times. Two points (normal condition and minimum boundary condition) on the linear curve combined with a known vessel resistance, fixes the maximum boundary condition: P_vCO_2 of 7.01 kPa corresponding to 0.376 times the default resistance. This makes that cerebral blood flow is already doubled at a P_aCO_2 of 6.7 kPa instead of 10.6 kPa, making our cardiovascular model more sensitive to increases in $[CO_2]_{dis}$, see figure 12 (dark blue curve). However, since the sigmoid shape and vertical axis of the curve corresponds to the curve show in literature, we have decided to not adjust the linear relation described above to optimise the maximum boundary condition.

Figure 13 (blue curve) shows the cerebral autoregulation curve, in case only the autoregulation mechanism is active in the cerebral circulation. Overcompensation of cerebral blood flow is seen, indicating that there needs to be some counteracting effect in order to maintain a stable flow between 50 and 55 mL/100g/min. As mentioned earlier, the autoregulation mechanism is not limited to the cerebral circulation. Systemic hypotension does not only affect the brain by a decline in intracranial blood supply, but all organs and tissues. Therefore not only vasodilatation of the small intracranial vessels is initiated to increase flow. In addition vasodilatation of extracranial small vessels is initiated to maintain adequate functioning of important organs, like the heart, kidneys and lungs.[12] It is assumed that the autoregulation mechanism of the extracranial circulation provides the counteracting effect preventing overcompensation of cerebral blood flow.

Definition of boundary conditions of the extracranial autoregulation mechanism is based on three assumptions:

1. Linear relation between $[CO_2]_{dis}$ and vessel resistance
2. In case of systemic hypo- or hypertension, boundary conditions are reached at the same time in the intracranial and extracranial circulation
3. The extracranial mechanism is weaker than the intracranial autoregulation mechanism

This leads to the following boundary conditions: minimum at a P_vCO_2 of 4.2 kPa corresponding to 1.84 times the default resistance value, and maximum at a P_vCO_2 of 7.2 kPa corresponding to 0.5 times the default resistance.

Figure 13 (red curve) shows the resulting cerebral autoregulation curve. For MAP between approximately 55 and 180 mmHg, cerebral blood flow remains quite stable: between 50 and 53.7 mL/100g/min during hypotension and between 50 and 58.4 mL/100g/min during hypertension.

Due to tissue metabolism, a constant amount of CO_2 molecules per time unit are produced in the intracranial ($1155 \cdot 10^{-6}$ mmol/ms) and extracranial tissues ($6630 \cdot 10^{-6}$ mmol/ms). As a result, arterial $[CO_2]_{dis}$ of 1.22 mM increases to venous $[CO_2]_{dis}$ of 1.41 mM. To remove the produced CO_2 molecules, 12.7% of the molecules are exhaled by the lungs. Both the tissue metabolism and oxygenation rates can be manually adjusted (both increase and decrease) in our cardiovascular model.

Table 7. Initial parameter conditions - the autoregulation mechanism.

Parameter	Initial condition	Remarks
CO_2 solubility (s)	0.0308 mM/mmHg or 0.231 mM/kPa	Solubility in blood plasma (37°C)
Partial arterial pressure CO_2 (P_aCO_2)	5.3 kPa	40 mmHg
Arterial CO_2 concentration $[CO_2]_{dis}$	1.22 mM	
Partial venous pressure CO_2 (P_vCO_2)	6.1 kPa	46 mmHg
Venous CO_2 concentration $[CO_2]_{dis}$	1.41 mM	
Intracranial autoregulation		
• Minimum boundary condition	P_vCO_2 4.35 kPa; 2.45x resistance	~2.5% blood loss
• Maximum boundary condition	P_vCO_2 7.01 kPa; 0.376x resistance	~5% blood excess
Extracranial autoregulation		
• Minimum boundary condition	P_vCO_2 4.2 kPa; 1.84x resistance	~2.5% blood loss
• Maximum boundary condition	P_vCO_2 7.2 kPa; 0.5x resistance	~5% blood excess
Normal brain tissue perfusion	50 to 55 mL/100g/min	sometimes 50 to 60 mL/100g/min[45]
Tissue metabolism (intracranial)	$117 \cdot 10^{-6}$ mmol/ms	~15%
Tissue metabolism (extracranial)	$663 \cdot 10^{-6}$ mmol/ms	~85%
Oxygenation rate	12.7%	~13%

THE CENTRAL NERVOUS SYSTEM (CNS) ISCHEMIC RESPONSE

Although the exact working mechanism of the CNS ischemic response is still largely unknown, its effect is assumed to be of major importance for the brain. The current theory implies that through a reduction of cerebral blood flow, the brain becomes ischemic. As a result of the ischemia, CO_2 and other acidic metabolites accumulate inside the brain tissue. Especially the increased $[CO_2]_{dis}$ provokes a sympathetic response in the cardiovascular control centre located in the medulla oblongata, leading to vasoconstriction of the venous blood vessels. By lowering the venous capacitance, venous vasoconstriction thus creates a blood shift from the venous system to the heart and arterial system. In this way, (cerebral) blood flow increases to remove the accumulated metabolites and to restore cerebral functioning.[12]

IMPLEMENTATION OF THE CNS ISCHEMIC RESPONSE INTO THE MODEL

Like the autoregulation mechanism, the CNS ischemic response is initiated by changes of local tissue $[CO_2]_{dis}$ in blood flowing from intracranial arterioles to the microcirculation & venous system. For similar reasons, average $[CO_2]_{dis}$ is taken over the last three heart periods. An increased $[CO_2]_{dis}$ (> 1.41 mM (or 6.1 kPa)) leads to a decrease of the venous capacitance, to promote venous return to the heart and thus intracranial blood flow. While a decreased $[CO_2]_{dis}$ (< 1.41 mM (or 6.1 kPa)) leads to an increase of the venous capacitance.

PARAMETER CHOICE - THE CNS ISCHEMIC RESPONSE

Just as the working mechanism is still rather unknown, no clinical or scientific data exists describing the working range of the CNS ischemic response. Therefore, we have chosen to use the same P_vCO_2 range as used

for the intracranial autoregulation mechanism: minimum boundary condition at a P_vCO_2 of 4.35 kPa and maximum at 7.01 kPa. Concerning the strength of the response; it turns out that the shape of the cerebral autoregulation curve (figure 13 (red curve)) is not affected by implementation of the CNS ischemic response. However, it does affect the ability of the cardiovascular model to compensate for distortions. To create the autoregulation curve of figure 13, MAP is varied by changing the total amount of circulating blood volume: volume reduction induces hypotension and volume enlargement hypertension. MAP and the corresponding cerebral blood flow were documented after reaching a steady state situation. If only the autoregulation mechanisms (both intra- and extracranial) are functioning, the minimum boundary condition is reached after removal of approximately 2.5% of total blood volume. For the maximum boundary condition, this was after adding approximately 5% of total blood volume. By assuming that venous capacitance becomes maximally 1.2 times the default capacitance value at a P_vCO_2 of 4.35 kPa and minimally 0.9 times the default condition at a P_vCO_2 of 7.01 kPa, up to 10% of total blood volume can be removed before reaching the minimum boundary condition. Furthermore, up to 20% can be added before reaching the maximum boundary condition. In conclusion, the range for which the cardiovascular model can maintain a stable cerebral blood flow increases by a factor four by implementation of the CNS ischemic response.

Table 3.8. Initial parameter conditions - the CNS ischemic response.

Parameter	Initial condition	Remarks
CNS ischemic response		
• Minimum boundary condition	P_vCO_2 4.35 kPa; 1.2x capacitance	~10% blood loss
• Maximum boundary condition	P_vCO_2 7.01 kPa; 0.9x capacitance	~20% blood excess

THE BARORECEPTOR RESPONSE

At strategic locations in the arterial vessels, pressure receptors or baroreceptors are located to regulate the MAP. The majority of these high-pressure baroreceptors can be found in the carotid sinus and aortic arch. The carotid sinus is a very distensible part of internal carotid artery vessel wall, located just above the bifurcation of the common carotid artery into the internal and external carotid artery. Since the aortic arch is also a very distensible part of the arterial vessel tree, it is not surprising that baroreceptors are stretch sensitive. Although they are also called pressure receptors, they are actually not pressure sensitive. Only direct stretching and thus deformation of the receptors, provokes a parasympathetic response in the cardiovascular control centre located in the medulla oblongata. As a result, both the heart and blood vessels are affected: an increased MAP leads to vasodilatation of extracranial blood vessels and bradycardia (increased HR) of the heart (parasympathetic response), while a decreased MAP leads to vasoconstriction of extracranial blood vessels and tachycardia (decreased HR) (sympathetic response).[12]

Besides high-pressure baroreceptors located in the high-pressure arterial system, low-pressure receptors are found in the low-pressure venous system detecting changes in venous pressure. These low-pressure receptors are located in the pulmonary artery, in the atria, at the junction of both atria and their corresponding veins and in the ventricles. Receptor deformation largely depends on the venous return and affects the effective circulating blood volume and CO. Thus low-pressure receptors are only an indirect regulator of MAP.[12]

IMPLEMENTATION OF THE BARORECEPTOR RESPONSE INTO THE MODEL

In this cardiovascular model we have implemented the high-pressure baroreceptors located in the carotid sinus. Due to our main focus on the intracranial circulation we have chosen for the receptors in the carotid sinus instead of those in the aortic arch. The low-pressure baroreceptors are disregarded, as their effect is secondary to that of the high-pressure receptors.[12]

Since baroreceptors are stretch sensitive, the pressure change over time *(dP/dt)* is determined each sampling interval in the intracranial small arteries (vessel compartment B). Due to the pulsatile pressure wave, the maximum *dP/dt* during the heart period is taken to initiate the baroreceptor response. Here again, to obtain a

gradual effect of the response, the average of maximal dP/dt values over the last three heart periods is determined. Running of the cardiovascular model using the initial parameter values, gives us a normal dP/dt value of 420 mmHg/ms. Furthermore, it shows that dP/dt does not increase linearly with the MAP, but curvilinear. Therefore the baroreceptor response is not described by a single linear curve, but instead by two linear curves with different slopes: one part below 420 mmHg and one part above 420 mmHg. An increase of dP/dt (> 420 mmHg/ms) measured in the small intracranial vessels, leads to vasodilatation of the small extracranial blood vessels to decrease cerebral blood flow. In addition, it leads to bradycardia of the heart, while a decrease of dP/dt (< 420 mmHg/ms) leads to vasoconstriction of the extracranial small vessels and tachycardia.

PARAMETER CHOICE - THE BARORECEPTOR RESPONSE

A normal HR is usually between 60 and 100 bpm. Tachycardia refers to a increased HR (> 100 bpm), while bradycardia refers to a decreased HR (< 60 bpm).[12] In this cardiovascular model we defined that a normal dP/dt of 420 mmHg/ms corresponds to a HR of 75 bpm. However, we assume that HR can increase linearly with a decreasing dP/dt towards 135 bmp, corresponding to 1.8 times the default HR. In addition, it can decrease linearly with an increasing dP/dt towards 45 bpm, corresponding to 0.6 times the default HR. This variation in HR from 45 to 135 bpm is quite comparable to a normal range seen in an untrained adult male person.[12] Since literature does not define minimum and maximum boundary conditions regarding dP/dt, we assume that the working range of the baroreceptor response is larger compared to that of the autoregulation mechanism. This assumption is based upon the fact that in contrast to the local autoregulation mechanism, the baroreceptor response regulates MAP (and thereby indirect (cerebral) blood flow) systemically. When the autoregulation mechanism reaches its limits, only two-third (66.7%) of the minimum (HR of 55 bpm) and maximum (HR of 115 bmp) conditions of the baroreceptor response are reached. This makes the final boundary conditions as follows: minimum at dP/dt of 0 mmHg/ms corresponding to a HR of 1.8 times the default value, normal condition at dP/dt of 420 mmHg/ms corresponding to the default HR, and maximum at dP/dt of 2000 mmHg/ms corresponding to 0.6 times the default HR value. The same dP/dt range is used to adapt the extracranial small vessel resistance. At this moment cerebral blood flow remains quite stable for MAP between approximately 50 and 180 mmHg: between 50 and 53.7 mL/100g/min during hypotension and between 50 and 58.4 mL/100g/min during hypertension (figure 13). However a normal range between 50 and 55 mL/100 during hypotension can be obtained by using the following minimum boundary conditions for the baroreceptor response: dP/dt of 0 mmHg/ms corresponding to 1.45 times the default resistance value. A similar effect during hypertension is obtained by using a maximum boundary condition: dP/dt of 2000 mmHg/ms corresponding to 0.45 times the default resistance value.

Table 9. Initial parameter conditions - the baroreceptor response.

Parameter	Initial condition	Remarks
Heart rate (normal range)	45 to 135 bpm	bradycardia <60 bpm tachycardia >100 bpm
Baroreceptor response (HR) • Minimum boundary condition • Normal condition • Maximum boundary condition	dP/dt 0 mmHg/ms; 1.8x HR dP/dt 420 mmHg/ms; 1x HR dP/dt 2000 mmHg/ms; 0.6x HR	~10% blood loss ~20% blood excess
Baroreceptor response (resistance) • Minimum boundary condition • Normal condition • Maximum boundary condition	dP/dt 0 mmHg/ms; 1.45x resistance dP/dt 420 mmHg/ms; 1x resistance dP/dt 2000 mmHg/ms; 0.45x resistance	~10% blood loss ~20% blood excess

PARAMETERISATION OF BLOOD FLOW VELOCITY

Apart from its educational purposes this cardiovascular model also provides insight into the new TCD parameterisation, defined by Schaafsma (Martini hospital, Groningen)[33,36] In order to calculate the four newly defined parameters (acc, sys1, sys2 and dias@560) accurately from the envelope curve of the raw TCD signal, software is developed in LabVIEW *(National Instruments, version 7.1.1)*. Currently this software is used in clinical practice in the Martini hospital and thus also during the observational prospective clinical study. The exact same software is implemented into the cardiovascular model, resulting in an equal parameterisation of the modelled blood flow velocity curve and the MCA blood flow velocity envelope measured in the septic ICU patients. Since the modelled signal is often much smoother than the raw signal measured in patients, some steps could have been left out. However we have chosen to use the exact same software in order to obtain comparable results.

Below a summary of the software algorithm used for parameterisation.

PRE-PROCESSING

Before the actual parameter calculation, the raw signal is pre-processed. Both the pre-processing and parameter calculation are performed over 10 second intervals, consisting of the latest 5 seconds added to the former 5 seconds, to obtain 100% overlap. This means that even during real-time simulation, analysis is performed off-line, creating a delay between the blood flow velocity displayed and the corresponding final parameter result. Since the software uses a default sample frequency of 250 samples/s, corresponding to the sampling frequency of blood flow velocity measured in septic ICU patients, the modelled flow velocity is down-sampled from 1000 samples/s (or eventually 500 samples/s) to 250 samples/s.

As the raw signals may contain high frequency fluctuations, a 10th order low-pass Butterworth filter with a cut-off frequency of 20 Hz is applied. Since pre-processing is performed off-line, a non-causal filter is used to avoid the non-linear phase delay of Butterworth filters. After the usual forward filtering, the filter output is turned back in time and filtered another time by the same filter. To get rid of eventual filter induced transient effects at the beginning and ending of each 10 seconds interval, the first and last 50 samples are removed.[46]

The choice to analyse 10 second intervals, is based on the fact that they contain multiple periodic beat-to-beat intervals with lengths corresponding to the heart period. This makes it possible to take an ensemble average over all the beat-to-beat intervals, to attenuate small fluctuations in blood flow velocity. In order to cut the 10 second interval into the individual heartbeats, we need to find the beginning of the beat-to-beat intervals. Interval's beginning is characterised by a rapid systolic upstroke, represented by a local maximum in the 1st order derivative, which becomes more prominent by squaring of the 1st order derivative. However, before squaring negative values are set to zero, to prevent confusion with fast decreases. For a first rough estimation of the interval beginning, the location is determined where the squared 1st order derivative crosses the following threshold: *mean + SD* of the squared 1st order derivative. Furthermore, time span between consecutive beat-to-beat intervals should always exceed 0.3 s, corresponding to the refractory period. To prevent a HR above 200 bpm, cardiac muscle cells cannot be excited during the refractory period.[47] However, the actual beginning of the beat-to-beat interval (systolic onset), is the location before the rough estimation, where the 1st order derivative equals 10% of the maximal acceleration. During cutting of the 10 seconds interval into the individual heartbeats, the first and last incomplete beats are not taken into account.

Amongst the beat-to-beat intervals deviating intervals can be found, resulting from technical artefacts (e.g. noise) or behaviour of the patient (e.g. couching, moving or talking). This will be especially the case for the raw signals measured in patients, and less for the modelled signals. As these deviating intervals are negatively influencing the ensemble average, removing of them leads to better representation of reality. Each individual beat-to-beat interval is compared to the mean of the remaining ones (reference signal). The L_2-norm or Euclidean norm of both the reference signal $\bar{f}$ as well as the deviation (individual signal (f) - reference signal ($\bar{f}$)) is calculated (Equation 26), to find deviating heartbeats.[48,49]

$$Euclidean\ norm\ reference\ signal\ \bar{f}$$

$$\left\| \bar{f} \right\|_2 := \sqrt{\frac{1}{N} \sum_{i=1}^{N} w_i \left(\bar{f}^2(t_i) \right)}$$

$$Euclidean\ norm\ deviation$$

$$\left\| f - \bar{f} \right\|_2 := \sqrt{\frac{1}{N} \sum_{i=1}^{N} w_i \left(f(t_i) - \bar{f}(t_i) \right)^2}$$

(26)

$N = number\ of\ samples$
$w_i = weighing\ factor$

A beat-to-beat interval is defined as deviating or an outlier according to equation 27.

$$\frac{Euclidean\ norm\ deviation}{Euclidean\ norm\ reference}\ or\ \frac{\left\| f - \bar{f} \right\|_2}{\left\| \bar{f} \right\|_2} > \alpha$$

(27)

Since the blood flow velocity of healthy individuals has on average an amplitude around 2 V, α is set on 0.2 V (10%). However, if the reference signal has an amplitude below 0.5 V, the deviation is only counted for 25% instead of 100%.

PARAMETER CALCULATION

After all these pre-processing steps, the ensemble average of the remaining beat-to-beat intervals is used to calculate the final parameters.

DIAS@560

When the shortest beat-to-beat interval is longer than 600 ms, the mean of the ensemble average is taken over the interval 520 to 600 ms after systolic onset. However, in case it is shorter than 600 ms, the last 80 ms of the shortest beat-to-beat interval are selected to determine the mean value. The reason to use the shortest beat-to-beat interval is due to the fact that hereafter ensemble average starts to decrease towards zero.

ACCELERATION (ACC)

The maximal increase in blood flow velocity per second is represented by a peak in the 1st order derivative. Since systolic upstroke lasts from the beginning of the beat-to-beat interval (systolic onset) until the first local maximum (period of about 0.1 s),[12] the highest peak during this interval is taken as acc value.

SYS1 AND SYS2 COMPONENTS

In order to accurately calculate the sys1 and sys2 components, regions of interest are selected to perform a targeted search within these regions. Both of the parameters are located in the systolic part of the flow curve: the sys1 phase generally corresponds to the first 140 ms after systolic onset and contains the systolic upstroke and first systolic peak, while the sys2 phase corresponds to the remaining part of systole up to the incisure and contains the second systolic peak.[36] The theoretical location of incisure is determined by equation 6. However, often there is a (small) difference between this theoretical and the actual location. Therefore, an interval (10% of the total samples) around the theoretical location is selected to search for a more reliable incisure location. Since the incisure is characterised by a local minimum, it corresponds to a zero-line crossing from negative to positive of the 1st order derivative. In case the selected search area does not contain a local minimum, the theoretical location becomes the final location of the incisure. However, in case one local minimum is found, this location becomes the final incisure location. While, if multiple local minima are found, the minimum closest to the theoretical location becomes the incisure location.

Clinical measurements show, that the sys1 as well as the sys2 component can gradually change from a clearly distinguishable peak into a shoulder to finally disappear. In case of a clearly distinguishable peak, its maximum is represented by a zero-line crossing from positive to negative of the 1st order derivative. However, in case of a

shoulder, higher order derivatives are needed to localize the shoulder. We have chosen to only use the 2nd order derivative in addition to the 1st order derivative and to exclude use of higher orders.

First the 1st order derivative is used to find both components by determining the locations where the derivative crosses the zero-line from positive to negative. If both the sys1 and sys2 components are located in their expected interval, the final values are found. However, if for example the sys2 component is not located in the sys2 phase, in addition the 2nd order derivative is used to find a possible sys2 shoulder. Parts of the sys2 phase are selected where the 2nd order derivative is negative, corresponding to a convex shape. In these parts the location is determined where the ensemble average has the highest value. This location becomes the final sys2 component. Generally, this location corresponds to a zero-line crossing from positive to negative. When there are no negative parts, the measured signal does not contain a sys2 component. A similar procedure is performed to find a sys1 shoulder. However, now the location generally corresponds to a zero-line crossing from negative to positive.

NORMALISATION

Finally, acc, sys1 and sys2 are divided by the dias@560 value to normalize the values and thus to make them independent of the insonation angle, cross sectional vessel area, HR, ABP, heart function and peripheral vessel resistance.

BLOOD LOSS OR BLOOD EXCESS

In septic patients it is of major importance to achieve a proper volume balance. Under-resuscitation should be prevented as it is associated with high mortality and morbidity rates.[50] Hypovolemia in septic patients may be caused by massive vasodilatation, transudation of fluid into the extravascular compartment, increased insensible fluid loss or decreased oral intake.[51] Preload optimisation by means of initial aggressive fluid resuscitation is highly recommended as first treatment step for septic patients to improve CO and ABP. On the other hand, fluid resuscitation should be strictly guided to prevent over-resuscitation[51–53] as this is too associated with increased mortality and morbidity.[51]

IMPLEMENTATION OF BLOOD LOSS OR BLOOD EXCESS INTO THE MODEL

To model the initial blood loss seen in septic patients and the effects of fluid resuscitation, it is in this cardiovascular model possible to adjust the total circulating blood volume of 5000 mL. By adjusting the percentage of blood loss or excess, the corresponding amount of volume is removed or added to the total circulating blood volume over a period of 30 seconds, to prevent oscillations. Of the total amount removed or added, 5% is removed or added to the volume in the isolated container representing the remaining heart volume, 10% to the volume in the isolated container representing the pulmonary circulation, and 85% to the volume in the microcirculation & venous system. Within a couple of seconds, the 85% of blood volume lost or administered via the microcirculation & venous system is proportionally redistributed over the entire systemic circulation.

REFERENCES

1. Van de Vosse FN, Stergiopulos N. Pulse Wave Propagation in the Arterial Tree. Annual Review of Fluid Mechanics. 2011 Jan 21;43(1):467-499.
2. Ku DN. Blood flow in arteries. Annual Review of Fluid Mechanics. 1997;29(1):399-434.
3. Quarteroni A, Formaggia L. Mathematical modelling and numerical simulation of the cardiovascular system. 2002 Jan.
4. Abdolrazaghi M, Navidbakhsh M, Hassani K. Mathematical Modelling and Electrical Analog Equivalent of the Human Cardiovascular System. Cardiovascular Engineering. 2010 Mar 9;10(2):45-51.
5. Timms DL, Gregory SD, Stevens MC, Fraser JF. Haemodynamic modeling of the cardiovascular system using mock circulation loops to test cardiovascular devices. Engineering in Medicine and Biology Society, EMBC, 2011 Annual International Conference of the IEEE. 2011:4301–4304.
6. Zhu KY, Ang A, Acharya U. R, Lim CM. Human Cardiovascular Model and Applications. Journal of Medical Systems. 2010 May 12;35(5):885-894.
7. F Fajdek B, Golnik A. Modelling and simulation of human circulatory system. Methods and Models in Automation and Robotics (MMAR), 2010 15th International Conference. 2010:399-404.
8. Kim HJ, Vignon-Clementel IE, Coogan JS, Figueroa CA, Jansen KE, Taylor CA. Patient-specific modeling of blood flow and pressure in human coronary arteries. Annals of Biomedical Engineering. 2010 Oct;38(10):3195-3209.
9. Westerhof N, Lankhaar J-W, Westerhof BE. The arterial Windkessel. Medical & Biological Engineering & Computing. 2008 Jun 10;47(2):131-141.
10. Shi Y, Lawford P, Hose R. Review of zero-D and 1-D models of blood flow in the cardiovascular system. Biomedical Engineering Online. 2011;10:33.
11. Sheffer L, Santamore WP, Barnea O. Cardiovascular Simulation Toolbox. Cardiovascular Engineering. 2007 Jun 15;7(2):81-88.
12. Boron WF, Boulpaep EL. Medical Physiology 2nd edition. Elsevier Saunders; 2008.
13. Reymond P, Merenda F, Perren F, Rufenacht D, Stergiopulos N. Validation of a one-dimensional model of the systemic arterial tree. AJP: Heart and Circulatory Physiology. 2009 May 8;297(1):H208-H222.
14. Saito M, Ikenaga Y, Matsukawa M, Watanabe Y, Asada T, Lagrée P-Y. One-dimensional model for propagation of a pressure wave in a model of the human arterial network: comparison of theoretical and experimental results. Journal of Biomechanical Engineering. 2011 Dec;133(12):121005.
15. Gabryś E, Rybaczuk M, Kędzia A. Blood flow simulation through fractal models of circulatory system. Chaos, Solitons & Fractals. 2006 Jan;27(1):1-7.
16. Swartz MA. The physiology of the lymphatic system. Advanced drug delivery reviews. 2001;50(1):3-20.
17. Chemla D, Plamann K, Nitenberg A. Towards new indices of arterial stiffness using systolic pulse contour analysis: a theoretical point of view. Journal of cardiovascular pharmacology. 2008;51(2):111-117.
18. Nichols WW, O'Rourke MF. McDonald's Blood Flow in Arteries: Theoretical, Experimental and Clinical Principles. 5th edition. Hodder Arnold Publishers; 2005.
19. Guarini M, Urzúa J, Cipriano A, González W. Estimation of cardiac function from computer analysis of the arterial pressure waveform. Biomedical Engineering, IEEE Transactions on. 1998;45(12):1420-1428.
20. Shiose A, Nowak K, Horvath DJ, Massiello AL, Golding LAR, Fukamachi K. Speed Modulation of the Continuous-Flow Total Artificial Heart to Simulate a Physiologic Arterial Pressure Waveform. ASAIO Journal. 2010 Sep;56(5):403-409.
21. Bárdossy G, Halász G. A "backward" calculation method for the estimation of central aortic pressure wave in a 1D arterial model network. Computers & Fluids. 2013 Mar;73:134-144.
22. Lankhaar J-W, Rövekamp FA, Steendijk P, Faes TJC, Westerhof BE, Kind T, et al. Modeling the Instantaneous Pressure–Volume Relation of the Left Ventricle: A Comparison of Six Models. Annals of Biomedical Engineering. 2009 Jun 25;37(9):1710-1726.
23. Westerhof BE. Quantification of Wave Reflection in the Human Aorta From Pressure Alone: A Proof of Principle. Hypertension. 2006 Sep 4;48(4):595-601.
24. Moran D, Epstein Y, Keren G, Laor A, Sherez J, Shapiro Y. Calculation of mean arterial pressure during exercise as a function of heart rate. Applied human science : journal of physiological anthropology. 1995;14(6):293-295.
25. Hudsmith L, Petersen S, Francis J, Robson M, Neubauer S. Normal Human Left and Right Ventricular and Left Atrial Dimensions Using Steady State Free Precession Magnetic Resonance Imaging. Journal of Cardiovascular Magnetic Resonance. 2005 Oct 1;7(5):775-782.
26. Cain PA, Ahl R, Hedstrom E, Ugander M, Allansdotter-Johnsson A, Friberg P, et al. Age and gender specific normal values of left ventricular mass, volume and function for gradient echo magnetic resonance imaging: a cross sectional study. BMC Medical Imaging. 2009;9:2.

27. Hill L, Gwinnutt C. Cerebral blood flow and intracranial pressure. Update in Anaesthesia. 2007:30-35.
28. Ito H, Kanno I, Iida H, Hatazawa J, Shimosegawa E, Tamura H, et al. Arterial fraction of cerebral blood volume in humans measured by positron emission tomography. Annals of Nuclear Medicine. 2001 Apr;15(2):111-116.
29. Hua J, Qin Q, Pekar JJ, Zijl PCM. Measurement of absolute arterial cerebral blood volume in human brain without using a contrast agent. NMR in Biomedicine. 2011 Dec;24(10):1313-1325.
30. McVeigh GE, Bank AJ, Cohn NJ. Arterial compliance. Cardiovascular Medicine, section VIII. Springer London. 2007:1811-1831.
31. Sawdon M. Characteristics of special circulations. Anaesthesia & Intensive Care Medicine. 2013 Feb;14(2):68-71.
32. Petzold LR, Ascher UM. Computer methods for ordinary differential equations and differential-algebraic equations. Siam; 1997 Dec.
33. Schaafsma A. Improved parameterization of the transcranial Doppler signal. Ultrasound in Medicine & Biology. 2012 Mar;38(8):1451-1459.
34. Dart AM, Kingwell BA. Pulse pressure - a review of mechanisms and clinical relevance. Journal of the American College of Cardiology. 2001;37(4):975-984.
35. O'Rourke M. Arterial stiffness, systolic blood pressure, and logical treatment of arterial hypertension. Hypertension. 1990 Apr 1;15(4):339-347.
36. PaR Technology Flyer; Current TCD Parametrization. [cited 2013 Nov]; Available from: http://www.neuromon.eu /index/php.
37. Neuromon BV - Home [Internet]. [cited 2013 Nov];Available from: http://www.neuromon.eu/index.php
38. Junqueira LC, Carneiro J. Functionele histologie. 11th edition. Elsevier gezondheidszorg; 2007.
39. Townsend P, Knowles MG. The cerebral circulation. Current Anaesthesia & Critical Care. 1999;10(2):77-82.
40. Bor-Seng-Shu E, Kita WS, Figueiredo EG, Paiva WS, Fonoff ET, Teixeira MJ. Cerebral hemodynamics: concepts of clinical importance. Arquivos de neuro-psiquiatria. 2012;70(5):352-356.
41. Panerai RB. Cerebral Autoregulation: From Models to Clinical Applications. Cardiovascular Engineering. 2007 Nov 28;8(1):42-59.
42. Aaslid R, Lindegaard KF, Sorteberg W, Nornes H. Cerebral autoregulation dynamics in humans. Stroke. 1989 Jan 1;20(1):45-52.
43. Strandgaard S, Paulson OB. Cerebral autoregulation. Stroke. 1984 May 1;15(3):413-416.
44. Arthurs G. Carbon dioxide transport. Continuing Education in Anaesthesia, Critical Care & Pain. 2005 Oct 14;5(6):207-210.
45. Care N. Principles of cerebral oxygenation and blood flow in the neurological critical care unit. Neurocritical Care. 2006;4:77-82.
46. Heida T, Meinsma G, van Putten MJAM. Syllabus for the course Advanced Techniques for Signal Analysis. University of Twente; 2010.
47. Moore KL, Dalley AF. Clinically Oriented Anatomy By Moore & Dalley. 5th edition. Lippincott Williams&Wilkins; 2005.
48. Rousseeuw PJ, Leroy AM. Robust regression and outlier detection. Wiley-IEEE; 2003.
49. Daszykowski M, Kaczmarek K, Vander Heyden Y, Walczak B. Robust statistics in data analysis - A review. Basic concepts. Chemometrics and Intelligent Laboratory Systems. 2007;85(2):203–219.
50. Wratten ML. Therapeutic approaches to reduce systemic inflammation in septic-associated neurologic complications. European Journal of Anaesthesiology. 2008;25(42):1-50.
51. Shujaat A, Bajwa AA. Optimization of Preload in Severe Sepsis and Septic Shock. Critical Care Research and Practice. 2012 Aug; E-pub 761051.
52. Dellinger RP, Levy MM, Carlet JM, Bion J, Parker MM, Jaeschke R, et al. Surviving Sepsis Campaign: international guidelines for management of severe sepsis and septic shock: 2008. Intensive care medicine. 2008;34(1):17-60.
53. Levitov A, Marik PE. Echocardiographic assessment of preload responsiveness in critically ill patients. Cardiology Research and Practice. 2012;2012:819696.